THESIS FOR THE DEGREE OF DOCTOR OF PHILOSOPHY

Lignins inside and outside the cell wall: Inherent and modified thermoplasticity

Åke Henrik-Klemens

Department of Chemistry and Chemical Engineering

CHALMERS UNIVERSITY OF TECHNOLOGY

Gothenburg, Sweden 2025

Lignins inside and outside the cell wall: Inherent and modified thermoplasticity
ÅKE HENRIK-KLEMENS

ISBN: 978-91-8103-348-9
Acknowledgements, dedications, and similar personal statements
in this thesis, reflect the author's own views.

Doktorsavhandlingar vid Chalmers tekniska högskola
Ny serie nr 5805
ISSN 0346-718X
DOI: https://doi.org/10.63959/chalmers.dt/5805

Department of Chemistry and Chemical Engineering
Chalmers University of Technology
SE-412 96 Gothenburg
Sweden
Telephone + 46 (0)31-772 1000

Cover: Artwork by Mats Mattson Broström. Oil on panel.
Printed by Chalmers Digitaltryck
Gothenburg, Sweden 2025

Lignins inside and outside the cell wall:
Inherent and modified thermoplasticity

ÅKE HENRIK-KLEMENS

Department of Chemistry and Chemical Engineering

Chalmers University of Technology

Abstract

Lignins are a group of irregular polyphenolic macromolecules found in vascular plants which, together with cellulose and hemicellulose, form highly robust materials. In the pulping process, individual wood cells are separated either by thermomechanical shearing or by chemically removing the lignified material that binds them together. Thus, from an industrial perspective there are three categories of lignin: native lignin in biomass, residual lignin in pulp and technical lignin extracted from biomass during pulping. This thesis concerns itself with all three categories of lignin, with the aim of understanding how the varying chemical structures of these lignins affect their properties – both inherent, and when modified for improved processability. It is especially the thermomechanical properties of these lignins that are in focus, as one of their potential uses is as thermoplastic components in biomass, in blends with synthetic polymers, or on their own. However, the glass transition temperature (T_g) of lignins is high, and their flow properties are poor due to the aromatic backbone, hindering thermal processing. But if the thermoplastic potential was realized, reliance on fossil-based thermoplastics could be overcome.

To investigate the thermomechanical properties, a powder sample holder for dynamic mechanical analysis (DMA) was employed, which allowed the determination of the T_g of isolated lignin as well as the T_g of *in situ* lignin in pulp and milled wood. By constructing Flory-Fox plots, the T_g could be compared beyond the effects of molar mass for the isolated lignins. Native structures appear beneficial for lower processing temperatures: residual lignin in softwood kraft pulp and softwood kraft lignin were projected to have a higher T_g at a given molar mass than native Norway spruce lignin. Upon modification with either external plasticizers or quantitative esterification ($C_{2\text{-}4}$), the response was uniform: external plasticizers were more efficient in reducing the T_g on a weight-addition basis for all lignins; however, the solubility of the plasticizers in the different lignins varied, with generally better compatibility with small flexible aprotic compounds. Additionally, plasticization was found to homogenize the physical properties of compositionally heterogenous lignins as well as increase coalescence of the otherwise brittle lignin materials.

Lastly, the external plasticization of softwood kraft pulp was investigated by probing which components the plasticizers were interacting with and their effect on the thermoformability of the cell wall. By employing optical photothermal infrared spectroscopy (O-PTIR) and solid-state NMR, plasticizers were found to be distributed throughout the fibers and interacting with all the major components – cellulose, hemicellulose and lignin. With DMA, the T_g of lignin was found to have dropped from around 230 °C to 120 °C. The plasticized pulp was hot pressed above and below this temperature, and the cell wall organization was investigated using X-ray scattering. Cellulose elements were found to aggregate; however, this was achieved without a reduction in crystallinity only in the presence of plasticizers and at higher temperatures. This indicates that the displacement mechanism for cellulose units during hot-pressing was more plastic when operating above the T_g of lignin.

Keywords: lignin, lignocellulose, kraft lignin, glass transition, plasticization, thermoformability

*"*They played a movement of Haydn, some pages of Mozart, a sonata of Beethoven. Then, while Gerda was picking out some music, with her violin under her arm, a surprising thing happened: Herr Pfühl, Edmund Pfühl, organist at St. Mary's, glided over from his easy interlude into music of an extraordinary style; while a sort of shame-faced enjoyment showed upon his absent countenance. A burgeoning and blooming, a weaving and singing rose beneath his fingers; then, softly and dreamily at first, but ever clearer and clearer, there emerged in artistic counterpoint the ancestral, grandiose, magnificent march motif – a mounting to a climax, a complication, a transition; and at the resolution of the dominant the violin chimed in, fortissimo. It was the overture to *Die Meistersinger."*

Buddenbrooks by Thomas Mann

List of publications

This thesis is based on the following appended publications and manuscripts:

I. The glass transition temperature of isolated native, residual, and technical lignin
Åke Henrik-Klemens, Fabio Caputo, Roujin Ghaffari, Gunnar Westman, Ulrica Edlund, Lisbeth Olsson, Anette Larsson
Holzforschung 2024, 78(4), 216-230.

II. Dynamic mechanical analysis of plasticized and esterified native, residual, and technical lignins: compatibility and glass transition
Åke Henrik-Klemens, Ulrica Edlund, Gunnar Westman, Anette Larsson
ACS Sustainable Chem. Eng. 2025, 13 (4), 1648–1656

III. Morphology and molecular mobility of plasticized lignins studied with polarization transfer solid-state NMR and X-ray scattering
Åke Henrik-Klemens, Tobias Sparrman, Linnea Björn, Alexandar Matic, Anette Larsson
Polymer testing 2025 151 (2025): 108942.

IV. Investigation of holocellulose, lignin, and plasticizer interactions and their effect on the thermoformability of plasticized kraft pulp studied by ssNMR, O-PTIR and SAXS/WAXS
Åke Henrik-Klemens, Stephanie Bachmann, Dinu Iuga, Anette Larsson
Submitted

Other publications

The following publications were published during my PhD studies; however, they are not appended to this thesis, as the content is not directly related to the aims of the thesis.

- **Henrik-Klemens, Å**., Ghaffari, R., Haraguchi, S. and Larsson, A., 2025. Glass transition temperature and mechanical damping of spruce lignin plasticized with methylimidazolium-based ionic liquids. *Industrial Crops and Products*, *228*, 120962.
- Jia, Y., **Henrik-Klemens, Å**., Persson, M., Holmberg, K. and Bordes, R., 2025. Cellulose nanocrystal stabilized beeswax dispersions for consolidation of encaustic paintings. *International Journal of Biological Macromolecules*, 144085
- Frasca, S., Katsiotis, C.S., **Henrik-Klemens, Å**., Larsson, A., Strømme, M., Lindh, J., Galkin, M.V. and Gising, J., 2024. Compatibility of Kraft Lignin and Phenol-Organosolv Lignin with PLA in 3D printing and assessment of mechanical recycling. *ACS Applied Polymer Materials*, *6*(22), 13574-13584.
- Korelc, K., Larsen, B.S., Heintze, A.L., **Henrik-Klemens, Å**., Karlsson, J., Larsson, A. and Tho, I., 2024. Towards personalized drug delivery via semi-solid extrusion: Exploring poly (vinyl alcohol-co-vinyl acetate) copolymers for hydrochlorothiazide-loaded films. *European Journal of Pharmaceutical Sciences*, *192*, 106645.

Contribution report

The author of this thesis has made the following contributions to the publications included:

I. **First author.** Initiated the concept and methodology and further refined in collaboration with co-authors. Performed most experimental work, except enzymatic hydrolysis performed by FC and fractionation of kraft lignin performed by RG. Analyzed and interpreted results in collaboration. Wrote the first draft of the paper. Revision was done in collaboration.

II. **First author.** Concept and methodology were developed in collaboration with co-authors. Performed all experimental work. Led the data treatment and analysis, with input from the co-authors. Wrote the first draft of the paper. Revision was done in collaboration.

III. **First author**. Led the development of the concept and methodology, with valuable input from the co-authors. Performed sample preparation and X-ray scattering measurements. TS performed NMR experiments. Performed data treatment and analysis with valuable input from co-authors. Wrote the first draft of the paper. Revision was done in collaboration.

IV. **First author**. Primarily developed the concept and methodology with feedback from the co-authors. Performed all experimental work except NMR experiments, which were performed by SB and DI. Performed data treatment and analysis with limited feedback from co-authors. Wrote the first draft of the paper. Revision was done in collaboration.

Abbreviations and symbols

Analytical techniques

ATR-FTIR	Attuned total reflectance Fourier transform infrared spectroscopy
CP	Cross polarization
DMA	Dynamic mechanical analysis
DSC	Differential scanning calorimetry
GPC	Gel permeation chromatography
HETCOR	Heteronuclear correlation
INEPT	Insensitive nuclei enhancement polarization transfer
O-PTIR	Optical-photothermal infrared spectroscopy
SAXS	Small-angle X-ray scattering
ssNMR	Solid-state nuclear magnetic resonance spectroscopy
WAXS	Wide-angle X-ray scattering

Other abbreviations

AGX	Arabinoglucuronoxylan
DEP	Diethyl phthalate
DMSO	Dimethyl sulfoxide
EMAL	Enzymatic mild acidolysis lignin
H	4-hydroxyphenyl
HSP	Hansen solubility parameters
G	Guaiacyl
GGM	Galactoglucomannan
GLY	Glycerol
LCC	Lignin carbohydrate complexes
MF	Microfibril
ML	Middle lamella
MWL	Milled wood lignin
P	Primary cell wall
p-CA	p-coumaric acid
PEG	Poly(ethylene glycol)
PMMA	Poly(methyl methacrylate)
S	Syringyl
S1-3	1st, 2nd and 3rd secondary cell wall
TA	Triacetin
USKP	Unbleached softwood kraft pulp

Symbols

CrI	Crystallinity index
E'	Storage modulus
E''	Loss modulus
E_a	Activation energy
M_n	Number average molar mass
M_w	Weight average molar mass
T_g	Glass transition temperature
T^H_1	Proton spin-lattice relaxation time
$T^H_{1\rho}$	Proton spin-lattice relaxation time in the rotating frame

Contents

1. Introduction

Without the evolution of lignin, higher plants would not be possible. Cellulose is an excellent structural component, but it was only when paired with lignin, that skyward heights were attainable. Lignin complements cellulose mechanically but also protects against UV radiation and microbiological attack, and aids in the transportation of water through the vascular system (Weng and Chapple, 2010; Pesquet et al., 2025). Thus, the utility of lignin for plants is clear; however, how useful lignin is for man is still an open question. Scientists try to break it down chemically to form new platforms or look for innovative ways to use its surface or bulk properties. But the question remains, is it fire brought down from Olympus, or just fuel for a fire?

In pulping, the aim is to separate wood into its cellular components: fibers. This can be done by chemically removing the lignified middle lamella that glues them together, or by thermomechanically ripping the fibers apart. Lignin inside the cell wall can then be further removed via chemical treatment, but there are environmental and economic advantages to keeping it in pulp. Thus, we have three types of lignin at hand: native lignin in untreated biomass, residual lignin in pulp and technical lignin extracted from biomass during pulping. These lignins differ in their chemical and molecular structure as decoupling and coupling reactions take place during processing (Froass et al., 1996). In this thesis, the terms chemical structure and molecular structure are used interchangeably, as they are closely interrelated in the case of lignin.

This thesis concerns itself with all three categories of lignins, with the aim of understanding how their varying structures affect their properties. It is especially the thermomechanical properties of these lignins that are in focus, as one of their potential uses is as thermoplastic components in biomass, in blends with synthetic polymers, or on their own.

As amorphous polymers, lignins are thermoplastic, but due to their aromatic backbone and strong secondary interactions, they have poor flow properties, and their glass transition temperature (T_g) is high. This means that lignins often need some kind of modification, either physical or chemical, prior to thermal processing. Modifications of the thermoplastic properties of technical lignins, due to their abundance and availability, have been extensively investigated (Parit and Jiang, 2020). In contrast, native and residual lignin have received considerably less attention. Moreover, there remains a lack of understanding regarding the extent to which insights gained from one type of lignin can be transferred to another.

The need to replace fossil-based plastics with bioplastics has sparked interest in the plasticization of pulp (Eliasson et al., 2023; Eliasson et al., 2025) and the thermal-processing of lignin-containing pulp and paper (Elf et al., 2025; Pettersson et al., 2017; Oliaei et al., 2021; Sanchez-Salvador et al., 2024). Lignin forms the largest amorphous domains in the fiber cell wall, stretching up to tens of nanometers (Terashima et al., 2009; Donaldson, 2022). In the unmodified cell wall, lignin restricts the movement of cellulose elements and transfers stress between them (Jin et al., 2015; Salmén et al., 2016), but upon pressing these materials above the T_g of lignin, more dense and plastic-like materials can be molded (Oliaei et al., 2020; Oliaei et al., 2021; Elf et al., 2025). These observations would suggest that lignin is flowable under such conditions, but does the softening of lignin allow for a different deformation mechanism inside the cell wall? Improved plastic deformability of the cell wall, including slippage of load-bearing cellulose elements, has been suggested to be crucial for improving the formability of pulp materials (Vishtal and Retulainen, 2014); however, too soft fiber materials from weak product (Afshariantorghabeh, 2024). Thus, lignin may function as a thermally activated component that imparts stiffness to the fiber at room temperature while enabling plastic deformation upon heating.

Water is an efficient plasticizer for carbohydrates (Back and Salmén, 1982), but its miscibility with lignin is limited (Elf et al., 2025) and steam generation can cause damage to fiber materials (Cavailles et al., 2024; Pintiaux et al., 2019). Thus, the plasticization of pulp using small non-volatile organic molecules is of interest, as these could surpass the performance of water, allowing for more advanced thermoformability of paper. The mechanical properties change greatly upon plasticization with compounds such as ethylene glycol and glycerol (Salmén et al., 1984; Eliasson et al., 2023), but there is a lack in mechanistic understanding: where is the plasticizer and what role does it play?

My doctoral work has been part of the *Vinnova* competence center *FibRe*, which, at the time I started, was aimed at developing understanding in the field of lignocellulosic thermoplastics, with a focus on fiber (pulp) materials with minimal modification. My project aligns with the center's second hypothesis: that modification of the amorphous phase in the pulp cell wall can unlock the thermoplastic potential of these materials.

One aim of this thesis has been to develop understanding concerning how lignin's chemical structure, transformed from its native state, via kraft pulping, to residual and technical lignin, influences its thermomechanical behavior. And, continuing from this, how plasticization changes those properties so that lignin can be processed as a thermoplastic component in materials. This aim is associated with the following hypothesis:

> **H1**: Lignins with different chemical structures will have different correlations between molar mass and T_g.
>
> **H2**: Lignins with different chemical structures will require different modifications to be efficiently plasticized (T_g reduction).

A second aim has been to study the interactions between plasticizers and the components of the pulp cell wall and their effect on thermoformability. This aim is associated with the following hypothesis:

> **H3**: Plasticizing lignin in lignin-containing pulp will enable a more plastic displacement of cellulose elements.

2. Background

2.1. Wood structure and components

Wood is composed of elongated cells, of which most are oriented in the growth direction. The main functions of these cells are to provide mechanical support, store nutrients, and transport fluids. Softwoods, needle-bearing trees, and the major focus of this thesis, are evolutionarily older than their leaf bearing counterparts, the hardwoods, and generally have a less diverse cell organization. In softwood, up to 90-95 % of the cells are long and sturdy cells called tracheids, commonly referred to as fibers (Sjöström, 1981).

The two softwood species used in this study, Norway spruce (*Picea abies*) and Scots pine (*Pinus sylvestris*), generally have long fibers: 2-4 mm with a diameter of about 20-50 μm. The fibers formed early in the year, when large quantities of fluids need to be transported to the crown, are termed earlywood and have large diameters and thin cell walls (2-4 μm), maximizing the lumen – the central channel for fluid transportation. Latewood has smaller diameters, thicker cell walls (4-8 μm), and smaller lumens. The lumens form networks via nanometer-sized channels called pits. These channels are covered by thin semipermeable membranes, which allow fluids to pass (Duchesne and Daniel, 1999; Hanley and Gray, 1994; Esteban et al., 2023).

The fiber cell wall is a hierarchical and multilayered structure (**figure 1**). The fibers are joined by an adhesive layer, termed the middle lamella (ML), which in softwood is 0.2-1 μm thick and consists of mainly lignin with some pectic compounds. Moving in from the ML the layers and their approximate thickness are as follows: primary layer (P, 0.1 μm thick), first secondary layer (S1, 0.2 μm), secondary layer (S2, 1-2 μm) and the inner layer (S3, 0.1 μm) (Sjöström, 1981).

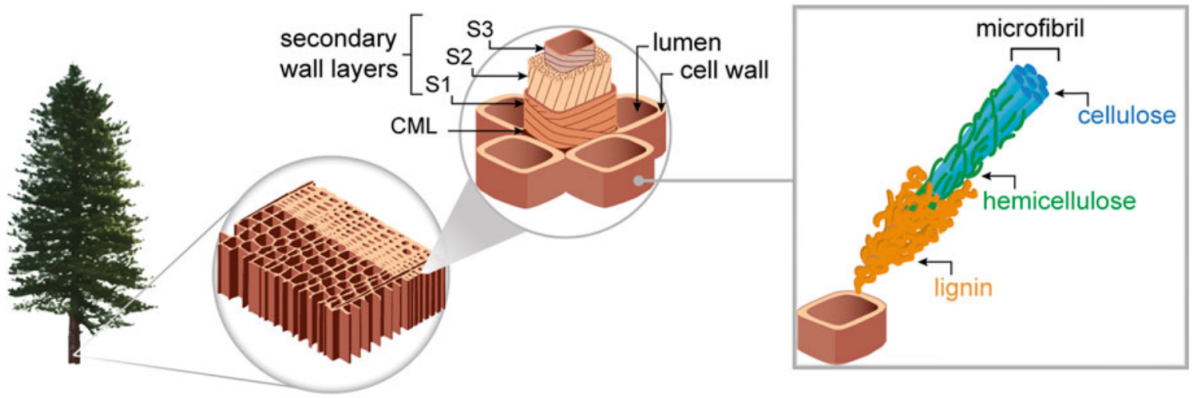

Figure 1. From macro to the nano-organization of the wood cell wall. Reprinted from (Montanari et al., 2021) licensed under CC BY. CML refers to the compound middle lamella, which also incorporates the primary cell wall layers.

The layers outlined above contain cellulose, hemicellulose, pectin, extractives and lignin, though with variations in composition and ordering. S2, which makes up the largest part of the cell wall, and has the most influence on its mechanical properties, has its cellulose microfibrils oriented longitudinally, but with an angle (typically 10-30° in softwoods)(Donaldson, 2008). This angle allows for both compression and extension to take place, without irrevocable damage. The microfibrils in P1 form an irregular interwoven network (Brändström, 2002), whereas microfibrils in S1 and S3 are oriented at a greater angle, to give strength in the transversal direction (Reza et al., 2017). The topic of cell wall ultrastructure will be revisited in more detail in section 2.1.3 when kraft pulp is discussed.

The cells and their connecting tissue consist mainly of three polymeric materials: cellulose, hemicellulose and lignin. Other compounds, such as pectin and various extractives and proteins, are also present in small amounts, but they are of little concern in this thesis. Cellulose and hemicellulose are polysaccharides whereas lignin is a polyphenol.

Cellulose is the main load carrying component of wood. It is a semi-crystalline and isotropic polymer of D-glucose. The glucose is joined by alternating β(1-4) glycosidic bonds, forming a linear chain (**figure 2**). Several cellulose molecules are secreted

simultaneously in the cell wall by terminal complexes, forming microfibrils (MF, sometimes also referred to as elementary fibrils or fibrils). MF are commonly described as consisting of a continuous crystalline core, with a disordered outer layer (Cosgrove et al., 2024). In softwoods, the dimensions of MF are about 3 nm in diameter, and the length is in the micrometer-range (Kesari et al., 2021).

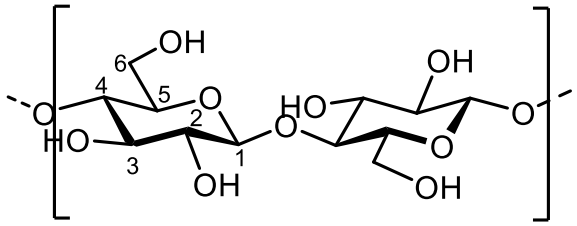

Figure 2. Structure of cellulose with carbon numbering. The repeating cellobiose unit consists of two β-D-anhydroglucose units.

In spruce, which is one of the most studied wood species, the number of chains secreted and making up the MF is still controversial; even though a consensus around 18 chains is forming (Jarvis, 2018; Daicho et al., 2025; Cosgrove et al., 2024), there is evidence for larger aggregates (Tai et al., 2023).

Hemicelluloses are less ordered and more varied in chemical structure compared to cellulose. In both Norway spruce and Scots pine, galactoglucomannan (GGM) and arabinoglucuronoxylan (AGX) are the two major hemicelluloses, comprising approximately 20 and 5-10 wt%, respectively (Bertaud and Holmbom, 2004; Sjöström, 1981). GGM consists of randomly distributed glucose and mannose units with galactose attached to the mannose via a 1-6 linkage. AGX has a backbone of xylose, but with glucuronic and arabinose side chains. Both hemicelluloses are linear with β(1-4) linkages and are partly acetylated (Berglund et al., 2020). The chemical structure of lignin will be dealt with in detail in later sections, but for now, conceptually, it can be regarded as an amorphous and irregular polyphenol.

2.2. The ultrastructure of the S2 in softwood and kraft pulp

As described in the previous section, MF are secreted in different patterns in different parts of the cell wall. The spaces between MF are then occupied by hemicelluloses and lignin which are polymerized in place. The organization of the hemi-lignin phase between cellulose elements is an area of much active research (Donaldson, 2019).

The occurrence of covalent bonds between the hemicelluloses and lignin, commonly termed LCC (lignin carbohydrate complexes), suggests that they are in close molecular contact (Sapouna and Lawoko, 2021; Giummarella et al., 2019; Lawoko et al., 2004), but in recent NMR studies they are found to possess different relaxation rates as well as limited through-space contact, suggesting different phases at the low-nanometer range (Kang et al., 2019; Terrett et al., 2019).

Salmén (2022) proposed a compelling model of the softwood S2 organization (**figure 3**), drawing in part on the above observations. According to this model, the MF are essentially coated with monolayers of hemicelluloses, with GGM primarily coating the surfaces between MF, and xylan located between the MF and the lignin phase.

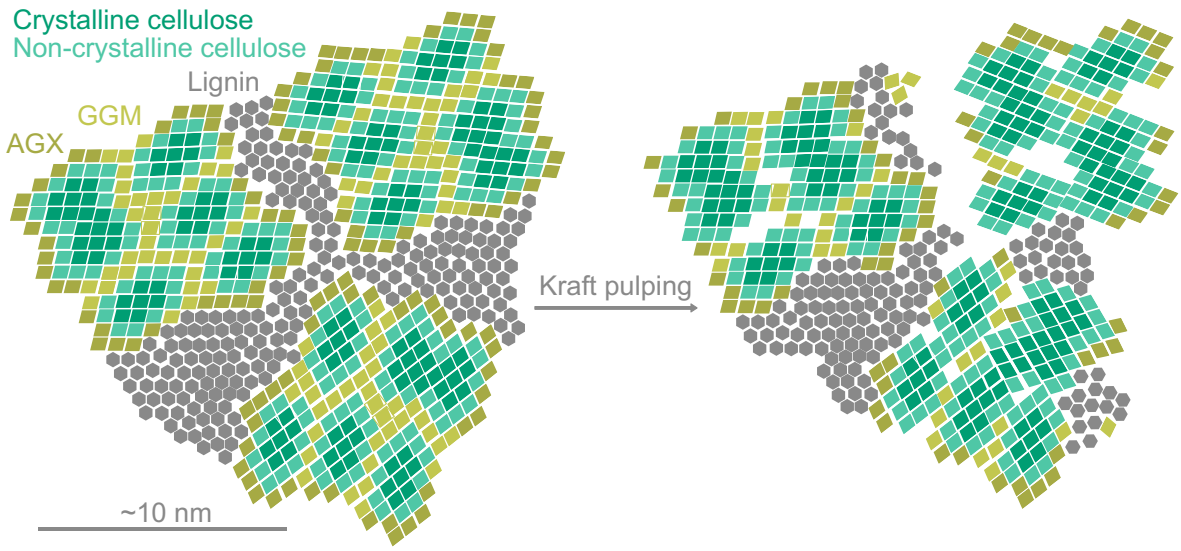

Figure 3. Illustration of softwood S2-layer in cross section before and after kraft pulping. The softwood S2 model is largely adopted from Salmén (2022), whereas the pulp S2 is based on the sources cited below as well as on the compositional and morphological analysis of the unbleached softwood kraft pulp used in this thesis. The MF bundles are here only shown in part with six MF in each. In contrast to wood, the pulp S2 sees a reduction in hemicellulose (mainly GGM) and lignin content, an increase in porosity, and aggregation of MF. The MFs are also in direct contact with lignin which has been redeposited to a certain extent; however, the exact extent and localization of these phenomena are not completely known, and the illustrations should be seen as idealized qualitative descriptions.

An early model on the organization of MF was put forward by Kerr and Goring (1975), which suggests radially lamellar structures, where the MF alternate between forming bundles and separating forming voids. This point of view has been strengthened in multiple later studies (Fromm et al., 2003; Ruel et al., 1978; Fahlén and Salmén, 2002). Both MF bundles and the lignin filled spaces between them have diameters between approximately 5 and 30 nm (Donaldson, 2022; Penttilä et al., 2020).

In a recent article, Fernando et al. (2023) used electron tomography to study the ultrastructure of the Norway spruce S2. By selectively removing lignin and labelling hemicellulose, they were able to differentiate the three components, as well as pore volumes. They found a non-lamellar, random distribution of the MF. The distribution and domain sizes described above hold relatively well, apart from the hemicelluloses, which were aggregated in larger nanometer domains.

We will now look at how the softwood S2 changes with kraft pulping. Kraft pulping proceeds by reacting wood chips under high temperature and high pressure with an alkaline water solution with the nucleophile, sulfide. The solution diffuses through the pits and fills the lumens, so that the reaction starts from the lumen outwards. A more detailed account of the reactions of lignins during kraft pulping is given in section 2.5 on technical lignin, but the main mechanism is fragmentation and dissolution (Espinoza-Acosta et al., 2014).

Depending on variables, such as time and temperature, pulps with varying lignin and hemicellulose content can be obtained. Some lignin is often redeposited on the fiber surfaces during pulping, influencing the formation of fiber joints (Li and and Reeve, 2005). Of the hemicelluloses, it is primarily GGM that is lost – the hemicellulose that serves as a barrier between MF (Henriksson et al., 2024). As a result, MF start to aggregate as well as come in direct contact with lignin (Salmén et al., 2016; Fahlén and Salmén, 2003; Duchesne et al., 2001; Liitiä, 2002).

The nature of the LCCs appears to change with pulping. Residual lignin in softwood has been found to retain more bonds to GGM than xylan (Lawoko et al., 2004). In hardwoods, there is evidence of both LCC formation and cleavage during kraft pulping (Nicholson et al., 2012; Nicholson et al., 2017). It is conceivable that the breaking and forming LCC bonds, and partial solvation of the amorphous cell wall compounds have led to more intermixing, or possibly, to aggregation of larger hemicellulose phases.

In the doctoral thesis by Liitiä (2002), she investigated the phase morphology of fines and isolated residual lignin using relaxation ssNMR. In the isolated residual lignin, the polysaccharide content was too low for accurate determinations of relaxation constants. But in the fines, both $T_{1\rho}^{H}$ and T_{1}^{H} (see section 3.4.3 for definition) could be determined for polysaccharides (mainly cellulose) and lignin. T_{1}^{H} of lignin and polysaccharide did not match in any of the fines analyzed (Liitiä et al., 2001); however, in some cases, $T_{1\rho}^{H}$ was found to match for both lignin and polysaccharides (Liitiä, 2002). The matching $T_{1\rho}^{H}$ and mismatching T_{1}^{H} of lignin and polysaccharides, suggest that at the local level, spanning a couple of nanometers, there is sometimes close contact between lignin and polysaccharides, but that they are separated at larger length scales. This suggests a system, where the interphases are partly either in close contact or moderately intermixed at the molecular level, while larger-scale phase separation is still present.

2.3. Micromechanical properties of the cell wall

A comprehensive micromechanical understanding of the pulp and wood cell wall has not yet been achieved, especially in the transversal direction, but based on molecular dynamics simulations, investigations of the cell wall organization and mechanical experiments, some general statements can be made.

The stiffness of cellulose is much greater than both lignin and hemicellulose (Zhang et al., 2021; Salmén, 2004); thus, as cellulose MF form a non-covalent interconnected network, large scale deformations require that the cellulose network is disrupted. Disruption can mean both reconfiguration of MF (straightening or curving) but also relative displacement (sliding or delamination), where the former is more elastic and the latter more plastic, as has been found when simulating S2 (Zhang et al., 2021; Jin et al., 2015) and primary cell walls (Zhang et al., 2025). The plastic deformation via sliding, termed stick-slip, has also been used to explain experimental data: the relaxation of MF in wood after straining them beyond the yield-point (Keckes et al., 2003).

The matrix polymers are important for the mechanical stability, as they both lock the network in place and, in the case of hemicelluloses, appear to increase cohesion between MF (Zhang et al., 2025). In the undulated cellulose network, stretching the cell wall in the fiber direction is resisted by the strong interactions of the cellulose bundles, but also as straightening of MF leads to a compression of lignin (Salmén et al., 2016).

The S2 layer is known to dominate the mechanical properties in the longitudinal direction; however, this is not necessarily the case in the transverse direction. In the latter, the nearly transverse orientation of MF in the S1 and S3 layers may play a more significant role (Reza et al., 2017; Donaldson, 2008). The organization of these layers is less studied, and their complex layering adds further challenges, which helps to explain why modeling the mechanical properties in the transverse direction have proven difficult (Salmén, 2018).

Water affects the components of the cell wall differently. The outer layer of cellulose can absorb water and swell, but it is hemicelluloses that absorb the largest amounts, causing significant swelling in wood and pulp. Water absorption separates polysaccharide chains, decreasing the energy cost of sliding elements across each other (Zhang et al., 2021; Jin et al., 2015; Zhang et al., 2025; Kulasinski et al., 2017). Lignin on the other hand absorbs a limited amount of water, leading to some softening and mobilization of lignin, but not to the same extent as the polysaccharides (Zhang et al., 2021; Vural et al., 2018b). The T_g of water-saturated cellulose and hemicellulose is typically found to occur around room temperature, whereas the T_g of water-saturated lignin plateaus at around 100 °C (Okugawa et al., 2023; Havimo, 2009; Åkerholm and Salmén, 2004; Back and Salmén, 1982; Kelley et al., 1987). In the next section, we will examine the molecular structure and properties of lignin, as well as the transformations it undergoes during the pulping process.

2.4. Native lignin

Lignin is a phenolic polymer with a lower hydrophilicity and lower degree of order compared to the wood polysaccharides, which allows it to both aid water transportation and protect against microbiological attack (Sjöström, 1981; Laschimke, 1989; Weng and Chapple, 2010). Lignin makes up about 25-35% of the dry mass of most woods (and 5-25 % in many monocots), but is unevenly distributed within the cell wall: the middle lamella contains the highest concentration, but due to the thickness of the S2 layer, most of the total lignin in wood resides there (Iiyama and Wallis, 1990; Rowell, 2013).

Lignin is an amorphous polymer made up of various phenylpropane-based monomeric units (**figure 4**). Its composition varies across plant types: softwood lignin is primarily composed of guaiacyl units, while hardwoods and monocots contain varying proportions of guaiacyl (G), syringyl (S), and 4-hydroxyphenyl (H) units (Tian et al., 2017; Pereira et al., 2017; Faleva et al., 2021). In its native form, lignin is synthesized through enzyme-initiated – though not enzyme-controlled – radical polymerization (Ralph et al., 2019). This process results in irregular polymer chains, with certain linkages occurring more frequently than others. Additionally, the radical mechanism leads to the formation of covalent bonds between lignin and carbohydrates, the previously discussed LCCs.

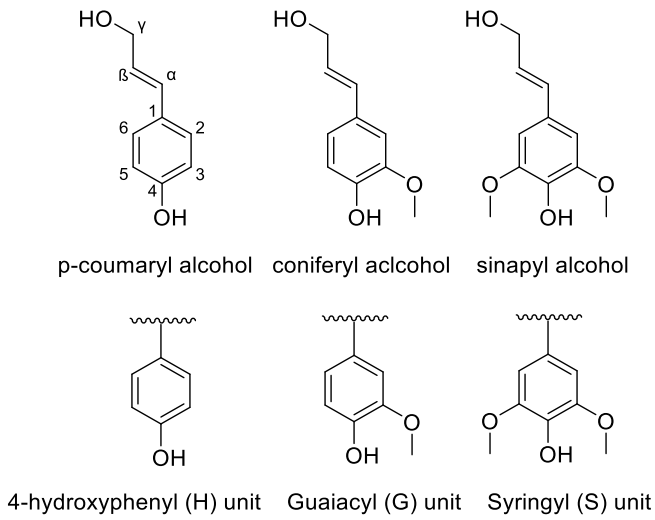

Figure 4. Chemical structure of lignin phenyl propane monomers (top) and respective lignol units (bottom). The conventional numbering and lettering scheme for lignol carbons is illustrated using p-coumaryl alcohol.

Among all plant types, the most prevalent linkage in lignin is the β-O-4 ether bond. This linkage occurs in roughly 80 % of aromatic units in monocot lignin, and in about 50 and 60 % in hardwood and softwood lignin, respectively (Zhang et al., 2022). **Figure 5** presents model structures of monocot and softwood lignins. These models illustrate the distribution of lignin monomers (H, G, and S units) and highlight common bonding motifs such as β-O-4, 4-O-5, and β-5 linkages. The models are not quantitative, but they offer an approximate visualization of native lignin macromolecules.

Monocot lignin has a larger diversity in building blocks than softwood lignin. Apart from the difference in lignol units H, G and S, monocot lignin also contains the flavonoid tricin and p-coumaric acid (p-CA). Polymerization of many monocots is believed to start with tricin, whereas p-CA is attached as a side chain (Ralph et al., 2019).

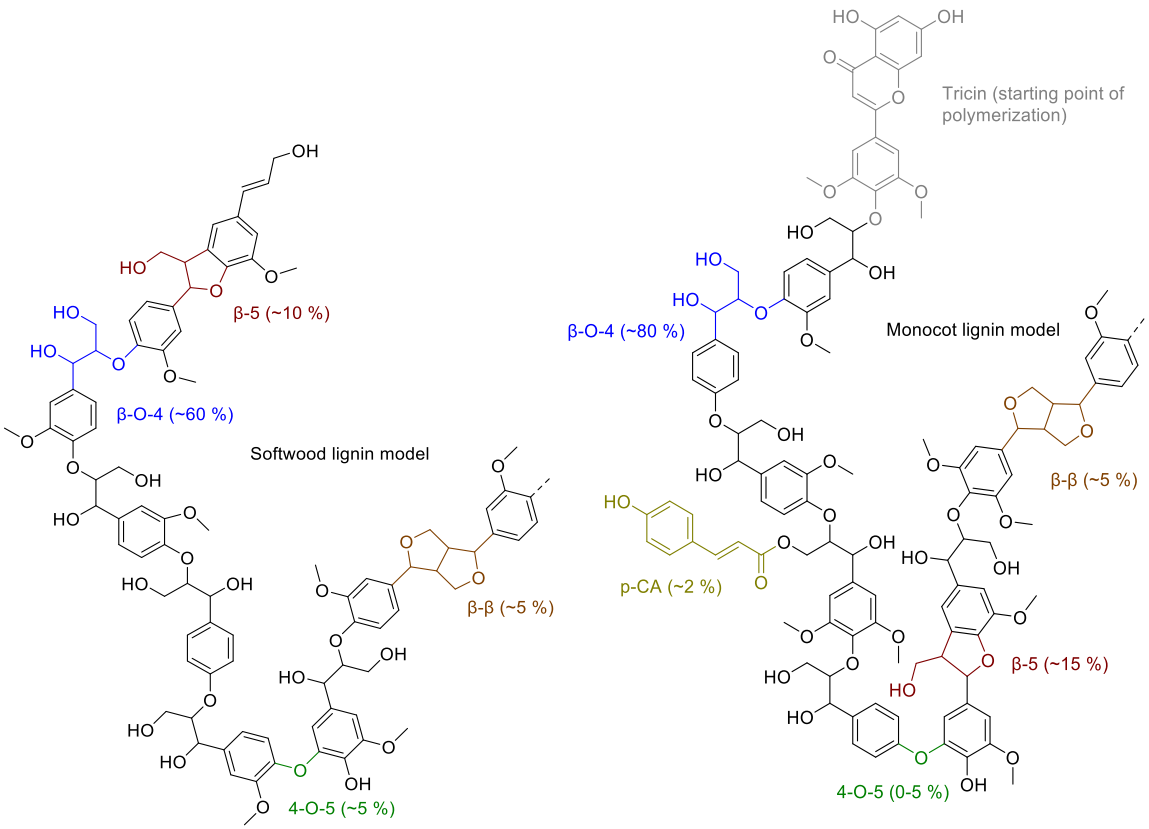

Figure 5. Softwood (left) and monocot lignin models (right), adapted from Ralph et al. (2019). The models are not to be seen as quantitative, but the approximate content per 100 aromatic units of certain linkages are given.

When Anselem Payen first isolated lignin in 1838, polymers were not yet a concept and lignin was believed to form a single crystal within trees (McCarthy and Islam, 1999). However, to this day, the molar mass of lignin in the cell wall is not known. This is partly due to the difficulty in isolating lignins and partly due to the experimental difficulty in the determining absolute molar mass of lignins (Souto and Calado, 2022).

2.5. Technical lignin

Technical lignins are those that are removed from biomass during pulping or other delignification processes. They are either named after their processing origin, such as kraft and organosolv lignin, or named after their chemical structure, such as lignosulphonates. Despite strong economic and environmental incentives to pursue higher-value applications, technical lignins are still commonly burned for energy (Jarnerö et al., 2024). In many respects, this situation is analogous to the early use of petroleum: a heterogeneous, polyaromatic resource that initially served primarily as a fuel before its chemical versatility unlocked vast commercial value.

The chemical structure of technical lignins varies depending on the raw material and on the delignification process, but they are often found to have a smaller molar mass than native lignin. This is because depolymerization is often needed for solubilization; which is typically achieved under either acidic or basic conditions, with or without an additional nucleophile. Depolymerization in most pulping processes is achieved by cleaving the abundant β-O-4 bond (Espinoza-Acosta et al., 2014). Kraft lignin, one of the focuses of this thesis, is solvated under high NaOH concentrations with sulfide acting as an additional nucleophile. An absolute method for determining lignin molar mass – gel permeation chromatography (GPC) coupled with multi-angle laser scattering – was used to determine number and weight average molar mass (M_n and M_w) of softwood kraft lignin (Zinovyev et al., 2018). They reported a M_n of 3.4 kg/mol and a M_w 16 kg/mol, corresponding to approximately 20 and 90 lignol units – significantly lower than the molar mass observed for analytically isolated native lignin with the same GPC system.

The majority of the native lignol linkages are broken during kraft pulping, but substantial coupling reactions also take place. Nucleophilic attacks by deprotonated phenols and alcohols are possible, but only lignin-carbohydrate ether bonds have been found in significant amounts, suggesting that it is not a major pathway (Crestini et al., 2017). Instead, coupling reactions via phenoxy radicals appear to be more

common, resulting in, e.g., 5-5' or 4-O-5 linkages. While the reaction mechanisms of many coupling reactions remain only partially understood and the structure of kraft lignin is not fully elucidated, these condensation reactions generally result in short atomic distances between the aromatic rings (Crestini et al., 2017; Balakshin et al., 2003; Gellerstedt and Zhang, 2001). In **figure 6**, a softwood kraft lignin model has been adapted from (Crestini et al., 2017).

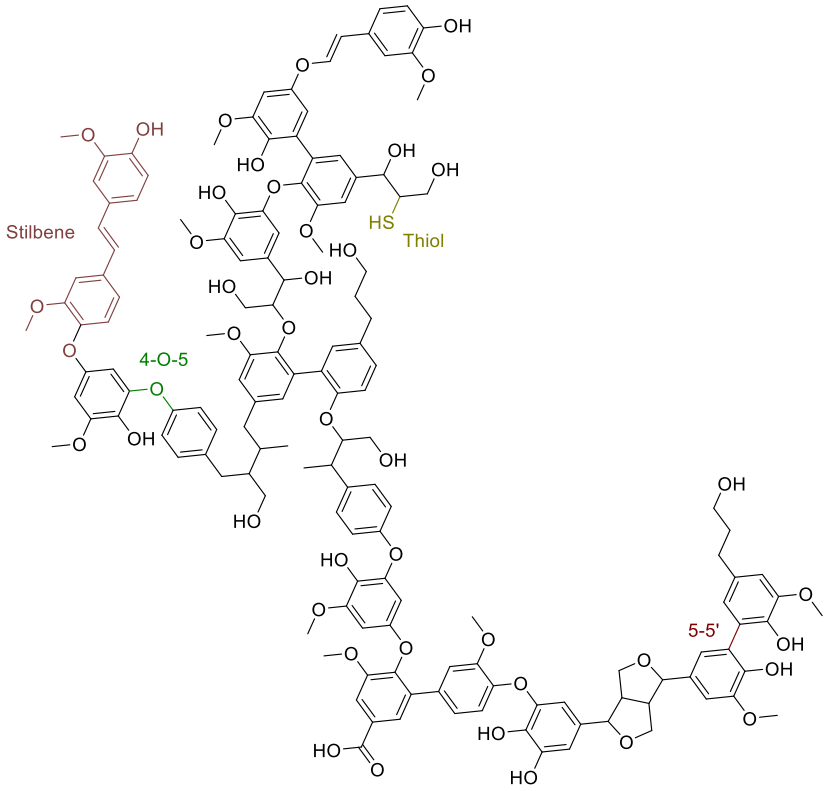

Figure 6. A model structure of softwood kraft lignin adapted from Crestini et al. (2017). The relative abundances of the various groups and bonding motifs are not specified, as they can vary considerably; however, 5-5' and 4-O-5 linkages are often among the most prevalent.

During kraft pulping, the hydroxyl group composition of lignin changes. The cleavage of β-O-4 linkages leads to an increase in phenolic OH groups, whereas the aliphatic OH content often decreases due to side-chain degradation reactions such as eliminations, oxidations, and rearrangements occurring under pulping conditions. (Crestini et al., 2017).

2.6. Residual lignin

Residual lignin, i.e. the lignin left in the fiber after pulping, has received less attention than its native and technical counterparts. Structurally, it is often found to be in-between, as it has intermediate phenol and alcohol content as well as both native and condensed linkages (Argyropoulos et al., 2002; Balakshin et al., 2003; Jääskeläinen et al., 2003; Froass et al., 1996); however, the absence of molar mass determination in many of these studies hampers comparison. It remains an open question whether it is condensation reactions during pulping which hinder depolymerization and solvation, or if it is the original structure of residual lignin that makes it resistant to pulping reactions.

2.7. The glass transition phenomena in polymers and in lignin

The glass transition is an important property of amorphous materials, such as polymers, but also for supercooled liquids such as glycerol. In polymers, large-scale movements of longer chain segments are restricted below the T_g, resulting in stiffness and elastic behavior. Above T_g, in the rubbery state, segmental mobility is possible, causing the material to soften and exhibit greater viscous behavior. For liquids, the glass transition is typically accompanied by a change in viscosity of more than 10 orders of magnitude (Ediger, 2000).

The glass transition is a phenomenon that is challenging to explain theoretically. It is not a first-order thermodynamic transition in the sense that it does not occur at a single, well-defined temperature at a given pressure – the transition temperature depends on the rate of temperature change, as well as on the frequency of the probing technique used. But the transition has easily measurable thermodynamic consequences: when going from the glassy to the rubbery state, the heat capacity of the material increases, as the degrees of freedom increase (Biroli and Garrahan, 2013; Cavagna, 2009).

One theory that explains the changes in polymer properties upon heating is the Free-volume theory. According to this theory, polymers occupy a certain volume, but there is also unoccupied space – known as *free volume* – between the polymer chains. Molecular movement can only occur when there is sufficient free volume to allow chain segments to shift into these spaces. Therefore, the amount of free volume in the system is a key factor in determining molecular mobility. At higher temperatures, free volume increases due to enhanced molecular vibrations, which expand the distances between chains. Below the T_g, the free volume is insufficient to permit large-scale chain mobility, whereas above T_g, segmental rearrangements become possible (Cavagna, 2009; Biroli and Garrahan, 2013).

The theory of Free volume is often good for predicting polymer behavior. An example of this is the Flory-Fox equation (**eq. 1**), which is an empirical relationship between molar mass and T_g, that has been interpreted with the concept of free volume. Chain segments have less free volume than chain ends, and therefore, M_n, which is a measure on the chain-end concentration, is inversely correlated to T_g (Fox and Flory, 1954; Fox and Flory, 1950).

$$T_g = T_{g,\infty} - \frac{K}{M_n} \tag{1}$$

where $T_{g,\infty}$ is the T_g at infinitely high M_n, and K is a constant related to the free volume in the sample and that relates M_n to T_g. Ogawa (1992) has offered a modified version of **eq. 1**, which considers the molecular-weight dispersity by replacing M_n with the geometrical mean of M_n and M_W, $(M_n M_w)^{1/2}$.

The free-volume theory, however, cannot fully account for all glass-forming phenomena. For example, some liquids have a drastic increase in viscosity upon approaching the glass transition without a change in density (Ferrer et al., 1998). The Adam-Gibbs theory takes better account of such phenomena, as it is built on cooperative dynamics: molecules or molecular segments form cooperative rearranging regions, which to relax, must cross local energy barriers (Adam and

Gibbs, 1965). Thus, it is the thermal energy in the system, and not packing, that dictates movement. This theory, as we shall see, also takes better account of how heterogeneous dynamics can arise in glassy materials, as properties between local regions may differ (Ediger, 2000).

With the development of polymer chemistry and physics in the post-war era, a new theoretical framework and toolbox became available to wood scientists, and in the 1960s, 70s, and 80s, there was a substantial interest in understanding the viscoelastic properties of lignin (McCarthy and Islam, 1999). Dry wood and pulp soften around or above 200 °C (Salmén, 1982; Startsev et al., 2017). Upon removing first lignin and then hemicelluloses, the softening lessens successively, but the onset temperature remains relatively unchanged (Salmén, 1982). As the corresponding isolated materials have T_gs in the same range (Goring, 1963), these transitions are likely a combinatory effect of either the cooperative or individual transitions of some of the amorphous wood components (lignin, hemi- and unordered cellulose). However, there is evidence for lignin having an individual glass transition not coupled with that of the polysaccharides (Kelley et al., 1987; Olsson and Salmén, 1997).

A major challenge in many early studies was the difficulty of isolating lignin in high yield while maintaining a structure representative of its native, *in situ* form. The isolated lignins typically exhibited T_g between 125 °C and 175 °C (Goring, 1963; Back and Salmén, 1982), significantly lower than those attributed to *in situ* lignin. This discrepancy is likely stemming from the low yield of the isolated fractions – typically only 10–30 wt% – which largely consisted of low molar mass components. In effect, such isolates can be considered a result of fractionation rather than the true representation of the whole lignin structure. The challenges associated with isolating representative lignin are further explored in the following section.

The structure-thermal property relationships of technical lignins have been widely studied due to their availability and central role in material development. Their T_gs typically fall between 100 and 160 °C, with kraft and soda lignins usually at the higher

end, while organosolv lignins tend to have lower T_g values (Wang et al., 2016). The lower T_g of organosolv lignins is could likely be attributed to efficient chain cleavage and low degree of recoupling reactions. Technical lignins often exhibit a high degree of heterogeneity, which is why they are frequently fractionated prior to further processing (Gioia et al., 2018; Karaaslan et al., 2021; Ebrahimi Majdar et al., 2019). In molar mass-fractionated lignins, T_g increases significantly with molar mass, following the Flory-Fox relationship (Ebrahimi Majdar et al., 2020; Yoshida et al., 1987).

2.8. Lignin isolation

The analytical isolation of lignin from the plant cell wall is one of the main challenges in lignin science. To accurately determine chemical structure and molar mass, isolation would ideally be both quantitative and non-degrading; however, the complex, hierarchical architecture of wood necessitates some degree of physical or chemical breakdown to access the lignin.

In an early attempt by Brauns (1939), about 10% of the lignin content was isolated from wood, by milling it to millimeter size and extracting with ethanol. Björkman (1956) was able to isolate 20-30% of the lignin from wood ball milled to a submillimeter powder, by extracting with dioxane with small additions of water. This latter method, known as Björkman's lignin or milled wood lignin (MWL), quickly became a standard protocol for isolating cell wall lignin, as it is considered to maintain much of the native molecular structure. Although the method has certain limitations – such as recovering only up to one-third of the lignin and inducing some depolymerization of wood polymers through ball milling (Sapouna and Lawoko, 2021) – it remains the most frequently and comprehensively studied lignin type, with data available from a wide variety of sources (Lupoi et al., 2015).

To avoid depolymerizing milling, techniques utilizing chemical degradation of the carbohydrate structure have been developed. In the 1950-60's, scientists managed close to quantitative isolation of lignin from wood degraded with fungi (Browning,

1967). A decade later, a more refined enzymatic treatment was developed, with similar yields (Polčin and Bezúch, 1978). A disadvantage of these techniques is that they entail high carbohydrate and protein contamination.

While many lignins, even those with relatively high molar mass, are soluble in solvents such as dioxane and dimethyl sulfoxide (DMSO) (Sameni et al., 2017), lignin-carbohydrate complexes (LCCs) tend to be less soluble and thus more difficult to isolate (Balakshin et al., 2014). Nonetheless, near-quantitative extraction of these complexes has been achieved using sequential dissolution in a series of solvents (Giummarella et al., 2019). Although this approach facilitates structural analysis of fractions, it should be noted that the bulk properties of these isolated fractions may not be representative of native lignin.

At the turn of the last century, a combination of these techniques (ball milling, enzymatic hydrolysis of carbohydrates and dissolution in acidified dioxane) was used to isolate lignins of high yield (~70 %) and a structure very similar to MWL (Wu and Argyropoulos, 2003). These lignins are termed enzymatic mild acidolysis lignin (EMAL). The utilization of ball milling, known to depolymerize lignins, and the acidified dioxane, used to break LCCs, are obvious disadvantages; nevertheless, this protocol has been used to isolate several types of lignin, and it is generally considered to provide a reasonable representation of the bulk properties in many respects (Argyropoulos et al., 2002; Jääskeläinen et al., 2003; Wu and Argyropoulos, 2003; Guerra et al., 2006b; Guerra et al., 2007; Asikkala et al., 2012). Though much attention has been given to the chemical and molecular structures of EMAL, their thermophysical properties have yet to be studied.

2.9. Plasticization of lignin and lignin-containing pulp

Due to the high T_g and poor flow properties of lignins, some modification is needed before thermal processing becomes possible, of which external plasticization is the simplest and most cost-effective. The first investigation into the external plasticization of lignin using small organic molecules was conducted by Sakata and

Senju (1975), focusing on two types of lignin: softwood thiol lignin (heavily condensed) and dioxane lignin (an isolated native lignin). The study examined the effects of three different types of plasticizers: phthalic, phosphoric, and aliphatic esters, with varying aliphatic chain lengths. Among these, phthalates were the most effective in reducing the T_g. Across all plasticizer types, shorter aliphatic side chains led to greater T_g depression, whereas molecules with chains of seven to eight carbon atoms ceased to act as plasticizers, likely due to phase separation. Both lignin types exhibited the same trend in response to side chain length; however, the study did not clarify whether they responded differently to the three types of plasticizers.

A wide range of compounds has been shown to reduce the T_g of technical lignin, provided they exhibit some degree of polarity (Ayoub et al., 2021; Banu et al., 2006; Milotskyi et al., 2019; Sakata and Senju, 1975). Bouajila et al. (2006) demonstrated that effectively lowering T_g requires saturation of the OH groups of lignin. In their study, water acted as a plasticizer only up to the point where the lignin-OH and H_2O were molar equivalent. Furthermore, acetylation of lignin – replacing OH groups with acetyl groups – lead to a T_g-reduction comparable to that achieved by adding an equivalent amount of water. These findings highlight the critical role of disrupting internal hydrogen bonding in decreasing lignin's T_g. An inverse correlation between lignin-lignin hydrogen bonds and T_g vs moisture content has also been found in molecular dynamics simulations (Elf et al., 2025; Vural et al., 2018a).

There has been some interest in looking at how different plasticizers affect the viscoelastic properties of *in situ* lignin (Sadoh, 1981; Miyoshi et al., 2018; Chowdhury and Frazier, 2013; Salmén, 1984). As previously stated, it is generally held that under saturated conditions, the T_g of the polysaccharide components of wood and pulp is around room temperature (Havimo, 2009), whereas the T_g of lignin remains around 100 °C. Generally, water, ethylene glycol, formamide and glycerol are good plasticizers for *in situ* lignin in wood, but DMSO, dimethyl formamide and N-methyl-2-pyrrolidone have been found to reduce the glass transition temperature

even further (Chowdhury and Frazier, 2013). The specific interactions have not been fully elucidated, but the aprotic nature appears important, and possibly, the solubility of the solvent/plasticizer in the lignin.

Changes in stiffness and strain at break were observed for both high-yield paper (Salmén et al., 1984) and bleached kraft pulp (Eliasson et al., 2023) when plasticized with ethylene glycol and glycerol, respectively. However, for the study on high-yield pulp, it was only upon heating that these changes were observed, and when delignifying the paper, the changes were much less pronounced. These findings suggest an intricate relationship between the mechanical properties of the papers, and the distribution and interactions of the plasticizers with the components of the pulp; however, the exact distribution of the plasticizers was never investigated.

Two compounds whose molecular distribution and interactions in wood and pulp have been investigated to a larger degree are water and poly(ethylene glycol) (PEG). Water is often described as being either free or bound, meaning either present in liquid form (in smaller or larger voids) or molecularly dispersed in the cell wall matrix, respectively (Thybring et al., 2022; El Hachem et al., 2020; Penvern et al., 2020). 2D relaxometry NMR has found that bound water occupies two distinct chemical environments in wood (Jeoh et al., 2017; Gezici-Koç et al., 2017). Given the spatial and chemical contrast between the lignin and polysaccharide-rich phases, it is likely that the two chemical environments bound water finds itself are represented by these, which Gezici-Koç et al. (2017) also suggest.

PEG is interesting as it is larger and less polar than water, and more like plasticizers of interest to this thesis. PEG in oligomeric sizes has been shown to penetrate the wood cell wall (Jeremic et al., 2007) via water submergence. In PEG impregnated archaeological wood, PEG has been found to both exist as phase separated and dispersed molecularly in lignin via ssNMR CP-kinetics experiments (Bardet et al., 2007). In a later study, penetration of the cell wall was again shown via Raman

microscopy, as well as the effective swelling of the amorphous matrix via SAXS (Penttilä et al., 2020).

Based on these previous studies on water and PEG, it appears reasonable to assume that the plasticizers used on pulp would distribute themselves in similar ways: molecularly dispersed in lignin, in polysaccharides or as a phase separated liquid. The two former would act as plasticizers, whereas the latter has potential as lubricant, hindering fiber-fiber joint formation (Vishtal and Retulainen, 2014). It is however interesting to note that water appears to distribute itself in both lignin and polysaccharide-rich phases, whereas PEG appears to largely interact with lignin – suggesting that selective plasticization is possible.

3. Methodology

3.1. Lignin isolation, fractionation, and characterization

To investigate the influence of chemical structure on the thermomechanical properties of lignins, lignins were isolated from Norway spruce, wheat straw, and unbleached softwood kraft pulp (USKP, composition in section 3.3) following the enzymatic mild acidolysis lignin (EMAL) protocol (Wu and Argyropoulos, 2003; Argyropoulos et al., 2002). The isolation process consists of three main steps: first, the biomass undergoes ball milling; second, holocellulose is enzymatically hydrolyzed; and finally, lignin is extracted using a mildly acidic dioxane solution (**figure 7**). A MWL was also isolated from Norway spruce. A more detailed description of the method is provided in **Paper I**.

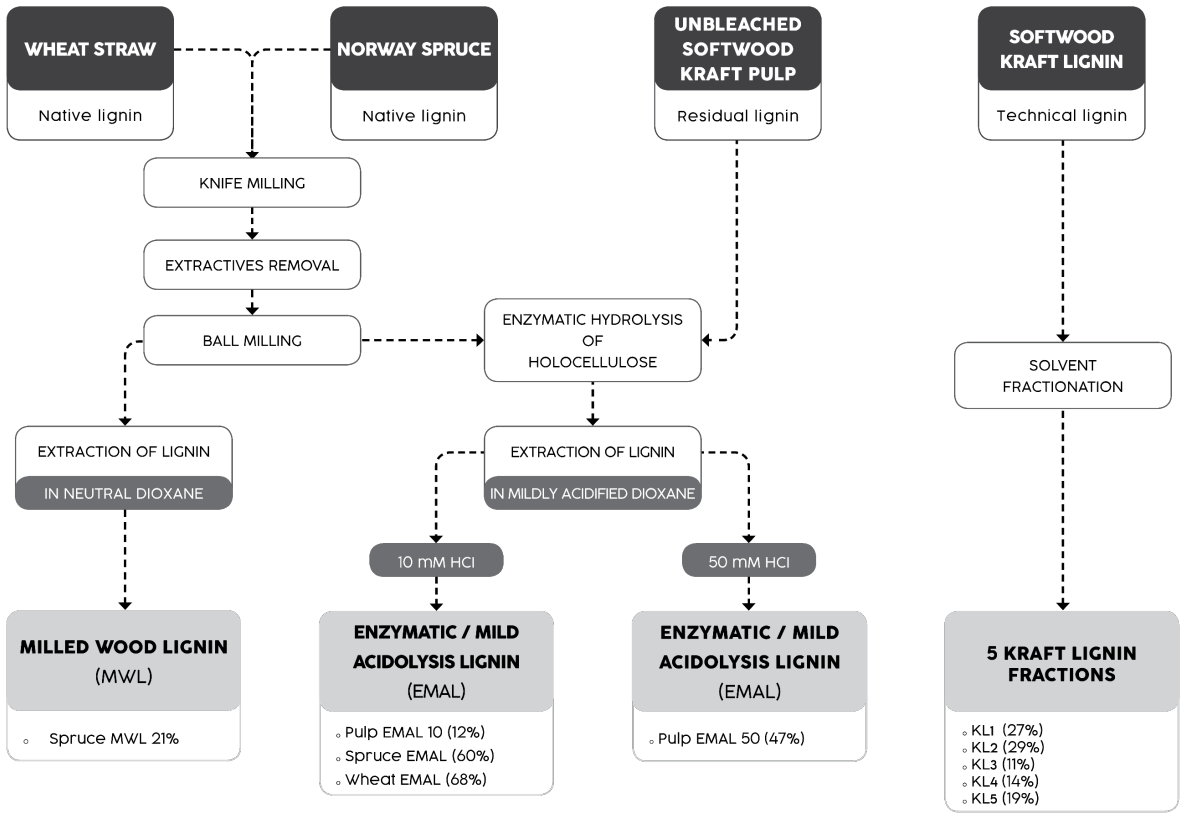

Figure 7. Isolation process. The value in parentheses is the yield of isolation (see **table 1** for details). The figure is adopted from **Paper I**.

Softwood kraft lignin (Lignoboost) was fractionated following the method described by Duval et al. (2016), which involves sequential dissolution in small volumes of different organic solvents: ethyl acetate, ethanol, methanol, and acetone. This approach separates the lignin into five distinct fractions, mainly characterized by different molar mass. Further details on the procedure can be found in **Paper I** and (Ghaffari et al., 2023).

These close-to-standard isolation and fractionation protocols have been used in this work to obtain established categories of lignin. Thus, characterization is mainly performed to confirm the success of the isolation of these categories, rather than for a full structural elucidation.

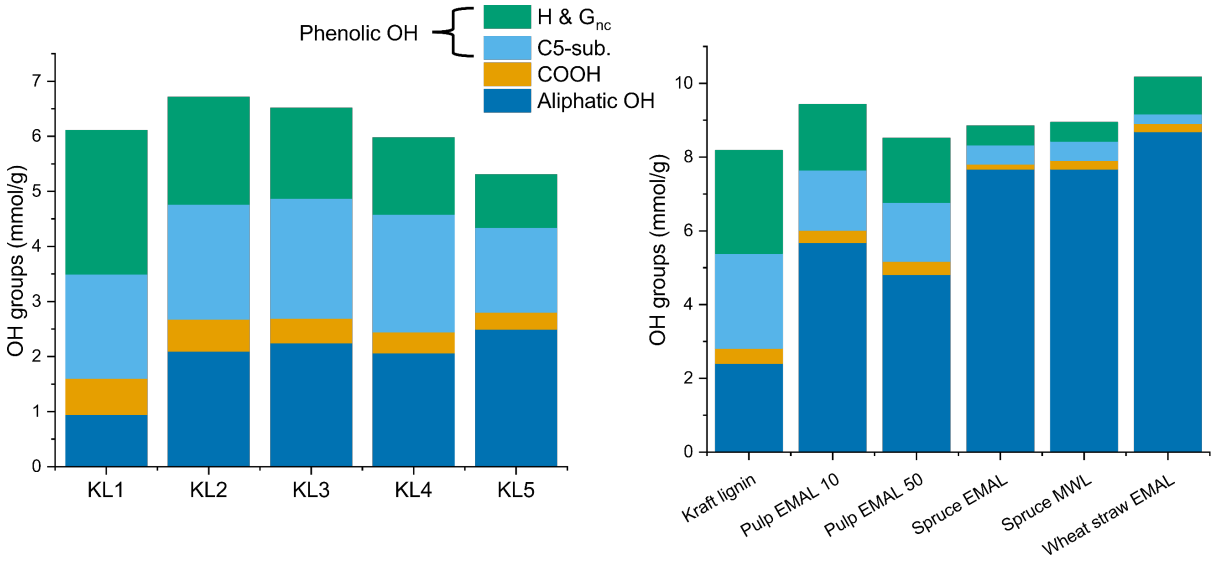

Figure 8. OH functional groups of kraft lignin fractions (left) and isolated lignins (right) determined with ^{31}P NMR according to Balakshin and Capanema (2015). Adopted from Paper I.

Details of the characterization are found in **Paper I**. In short, molar mass distribution was determined using pullulan-calibrated GPC in DMSO with 10 mM LiBr. Although pullulan calibration in DMSO tends to underestimate the size of lignin, this underestimation is linear, allowing for consistent comparisons within the same study (Zinovyev et al., 2018). See **table 1** for results. Hydroxyl group quantification was performed through ^{31}P NMR analysis of phosphorylated lignin, following the method described by Balakshin and Capanema (2015) (**figure 8**).

Table 1. Yield, molar mass, and purity of lignins.

Lignin (abbreviation)	**Yield**	M_n (kg/mol)	M_w (kg/mol)	**Purity**[c]
Spruce MWL	21%[a]	2.8	7.2	95.2% (0.4)
Spruce EMAL (SL)	60%[a]	3.8	27.5	92.6% (0.2)
Wheat straw EMAL (WL)	68%[a]	3.1	15.7	93.2% (0.4)
Pulp EMAL 50 (PL)	47%[a]	5.8	77.3	93.7% (0.1)
Pulp EMAL 10	12%[a]	4.7	37.0	90.3% (0.5)
Kraft lignin (KL)	-	1.6	12.2	93.5% (0.6)
KL1	27%[b]	0.7	1.8	-
KL2	29%[b]	1.9	5.4	-
KL3	11%[b]	2.6	6.1	-
KL4	14%[b]	6.8	13.4	-
KL5	19%[b]	14.8	42.5	-

[a]Yield = mass of extract/mass of Klason and acid soluble lignin of biomass.

[b]Yield = mass of extract/sum of the mass of all fractions.

[c]Purity = (Klason and acid soluble lignin - ash content - protein contamination)/mass of sample. Values in parentheses are the pooled standard deviations (n=3). See Paper I for details.

The results in **table 1** and **figure 8** confirm the expected structures discussed in section 2.4-2.6: the molar mass increases following technical<native<residual lignin, whereas phenol content increases native>residual>technical lignin. The KL fractions successively increase in molar mass (with relatively large dispersity) and relatively uniform OH composition (KL1 and KL5 differentiate somewhat). Wheat straw and Norway spruce EMAL also differ as expected, with a higher diversity of constituents in the former (**Paper I**). For **Paper III** and this thesis, CP ^{13}C NMR relaxation experiments were carried out to investigate the phase morphology of Spruce EMAL, kraft lignin and Pulp EMAL 50, which will be discussed later, but their respective spectra can be found in **figure 9**. The relative amount of aromatic (160-100 ppm) against aliphatic carbons (100-0 ppm) shifts successively (from native to residual to technical), demonstrating the loss of side chains during kraft pulping as discussed in section 2.5. The shift in increasing $G_{5\text{-}5'}$ follows the same trend,

indicating condensation reactions. A deeper analysis of the representativity of the lignins can be read in the first results section of **Paper I**, but by large, the isolated lignins represent their respective categories well.

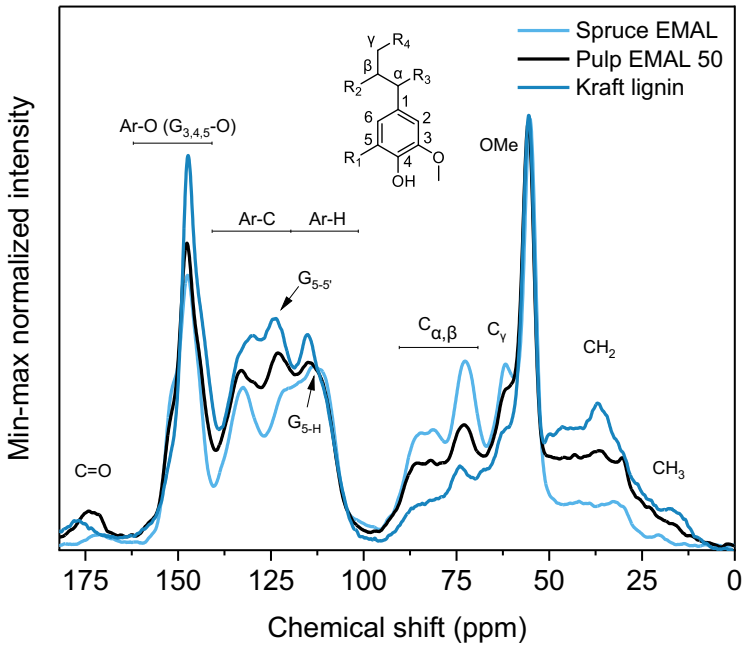

Figure 9. CP ^{13}C spectra of three softwood lignins with some general assignments based on (Hawkes et al., 1993).

3.2. Lignin modification

Four lignins were chosen for further modification based on the disparity in their chemical structure: spruce EMAL (SL), wheat straw EMAL (WL), pulp EMAL 50 (PL) and kraft lignin (KL).

3.2.1. External plasticization

These lignins were plasticized with glycerol (GLY), triacetin (TA) and diethyl phthalate (DEP) (**figure 10**. For procedure, see **Paper II**). The plasticizers were selected based on their functional groups, where GLY is protic, TA and DEP are aprotic, and DEP is aromatic. GLY can both donate and accept hydrogen bonds, whereas the other two can only accept. The electron deficient aromatic ring of DEP could also potentially interact with the electron rich aromatic ring of lignin, competing with its π-π stacking (Hackenstrass et al., 2025; Martinez and Iverson, 2012).

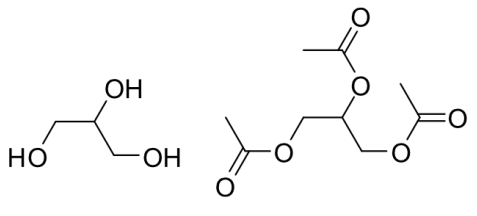

Plasticizer	Glycerol (GLY)	Triacetin (TA)	Diethyl phthalate (DEP)
Molecular weight	92 g/mol	218 g/mol	222 g/mol
$T_{g,DSC}$	-83 °C	-71 °C	-89 °C

Figure 10. Molecular structure, weight and T_g of plasticizers. The T_g of the plasticizers was determined with differential scanning calorimetry (DSC) (**Paper II**).

3.2.2. Lignin esterification

Lignins were esterified with acetic, propionic and butyric anhydride by adopting a method developed for quantitative acetylation of lignins for analytical purposes (Månsson, 1983). The success of the esterification was evaluated with attuned total reflectance Fourier-transform IR (ATR-FTIR) and ^{31}P NMR. IR found a close to

complete loss of OH stretching and the appearance of phenyl and alkyl esters (Faix et al., 1994) (**figure 11**). NMR confirmed the degree of esterification to about 94-100 wt%; however, some remaining acid impurities were also found (0-5 wt%. See **Paper II** for details).

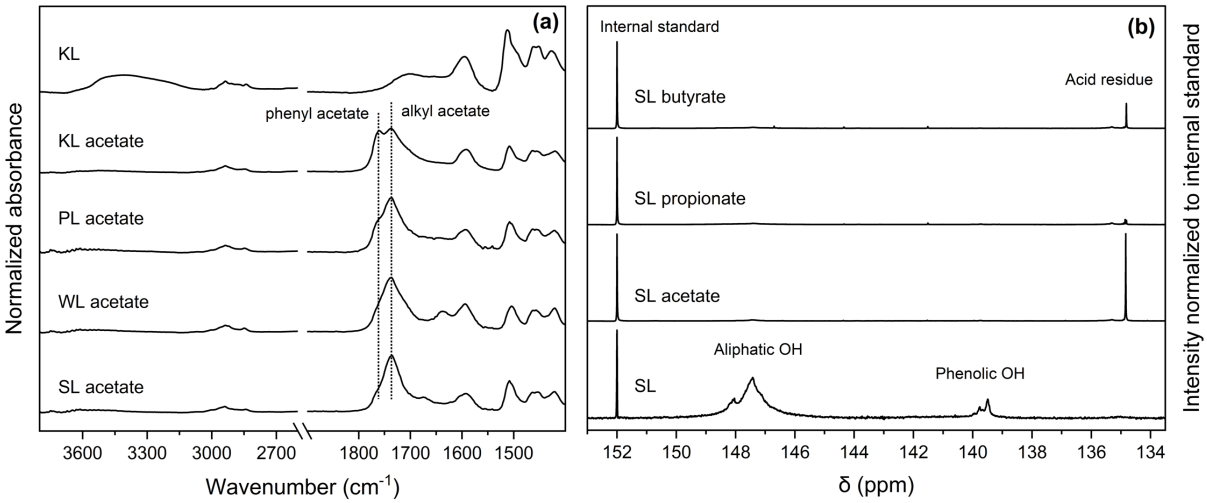

Figure 11. ATR-FTIR spectra of acetylated lignin normalized to the aromatic stretching at 1509 cm^{-1} (left) and ^{31}P NMR spectra of esterified SL (right). The figure is adopted from **Paper II**.

3.3. Pulp modification and characterization

The pulp used in this thesis was an unbleached softwood kraft pulp (USKP) made of an unknown ratio of Norway spruce (*Picea abies*) and Scots pine (*Pinus sylvestris*). The pulp was kindly supplied as never-dried by Stora Enso, who also carried out compositional analysis (**Paper IV**, **table S1**): 13 % lignin and approximately 10 % GGM and 9 % AGX.

The pulp was plasticized by suspending the never-dried pulp in water solutions containing 1-5 wt% of plasticizer (**figure 12**). The ratio of plasticizer to pulp ratio varied between 1:2 and 1:10, resulting in pulps of varying plasticizer content. The suspensions were heated to 50 °C and stirred vigorously for 48 hours to achieve dynamic equilibrium. For details on clean-up procedure, see **Paper IV**.

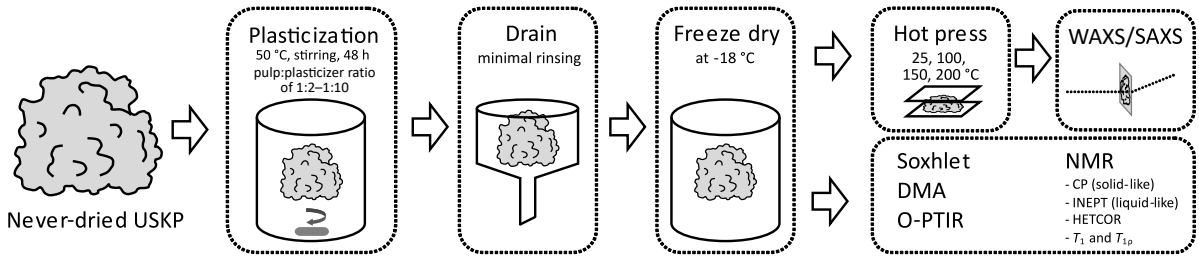

Figure 12. Plasticization of pulp and following characterization.

3.4. Characterization techniques

The unmodified and modified pulps and lignins were characterized using a range of techniques, with the three most relevant to this thesis – DMA, SAXS/WAXS, and NMR – described in the following sub-sections.

3.4.1. DMA

In DMA, a sample is subjected to a sinusoidal stress (σ), and the phase lag (δ) between the applied stress and the resulting strain (ε) is measured. In a purely elastic material, deformation occurs immediately when stress is applied, whereas viscous deformation causes a delay in the material's response. Based on the phase lag, the dynamic modulus can be divided into one elastic ($E' = \sigma_0/\varepsilon_0 \cos\delta$) and one viscous component ($E'' = \sigma_0/\varepsilon_0 \sin\delta$), where ε_0 is the maximum stress, ω is the frequency of the oscillation, and t is the time. The elastic modulus (E'), or storage modulus, represents the energy stored elastically in the material during deformation, while the viscous modulus (E''), or loss modulus, reflects the energy dissipated through viscous deformations. In older instruments, the primary output was the tangent of the phase lag, known as tan δ or tan delta, which remains frequently cited in the literature (Menard, 2008). This value is often interpreted as the fraction of viscous over elastic deformation, i.e. a measure on molecular motion.

The glass transition is characterized by a drop in storage modulus E', as illustrated in **figure 13**, indicating a reduction in the material's resistance to elastic deformation. Conversely, the loss modulus E'' forms a peak at the glass transition, (as does tan δ), that eventually plateaus at a lower magnitude. These peaks arise because energy

dissipation is maximized at the glass transition, where there is sufficient chain mobility to allow deformation, but the material still exhibits significant internal resistance. All these three definitions of the T_g ($T_{g\ E'\ onset}$, $T_{g\ E''\ max}$ and $T_{g\ \tan\delta\ max}$) will be used in this thesis. The maximum of E'' is sometimes preferred, as it is suggested to be more directly related to the transition to freer molecular movement (Hagen et al., 1994).

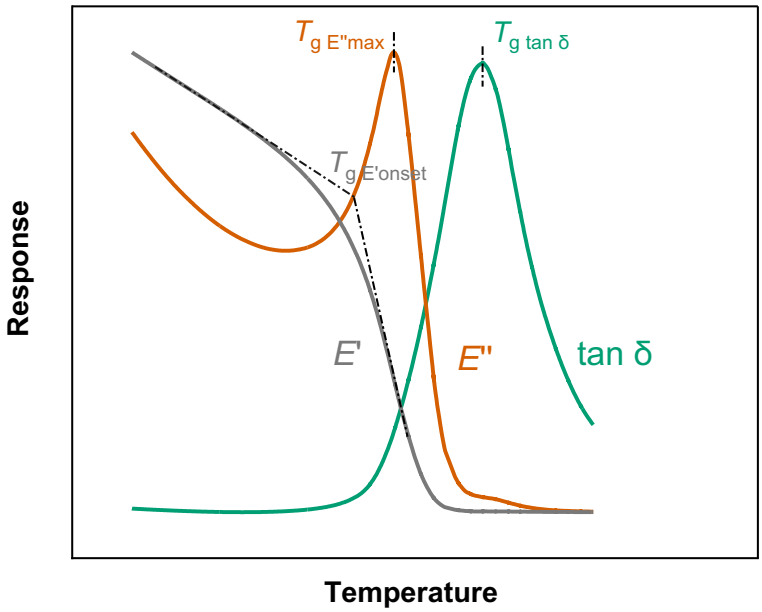

Figure 13. Schematic DMA thermogram illustrating the glass transition of an amorphous polymer.

Most isolated lignins cannot be cast or molded into continuous shapes, making them incompatible with standard DMA setups. Likewise, pulp that is not to be prepared as a paper will be difficult to measure as well. Over the past two decades, the development of powder sample holders has made it possible to analyze these kinds of non-continuous samples (**figure 14**). However, because the steel of the holder is strained along with the powder and the geometry factor is not well-defined, the moduli are non-absolute. Despite this, these setups have been shown to provide reliable and accurate determination of thermal transitions (Mahlin et al., 2009).

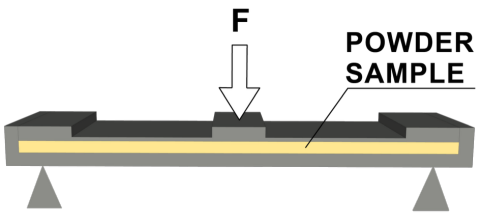

Figure 14. Illustration of powder sample holder for DMA (adopted from Henrik-Klemens (2023).

The DMA measurements in **Paper I** and **II** were performed on a Q800 (TA instruments) with liquid nitrogen cooling. In **Paper IV**, the measurements were performed on DMA 850 (TA instruments) with a cooling accessory and ventilation, which allowed high-temperature runs. The standard measurement on lignin was performed from 25 °C to 50 °C above the $T_{g\,E''}$, or as high as was possible before the sample started off gassing. Pulp samples were run up to 300 °C. A heating rate of 3 °C/min was applied to all samples. Lignins and pulp samples were run with a strain of 5 and 10 μm, respectively, with a frequency of 1 Hz. Unmodified lignin and all pulp samples were run with an annealing of 5 min at 120 and 80 °C, respectively, to remove moisture. Plasticized and acetylated lignins could not be annealed, as many of the samples started to flow out of the holder at higher temperatures, resulting in non-comparative force readings. However, samples ran with and without annealing had very similar transition temperatures, so the moisture content (typically around 3 wt%) did not appear to affect the modified lignins very much. The moduli values are non-absolute, but relative comparisons are possible. To enable this, E' are max-normalized.

The apparent activation energy (E_a) of the glass transition was determined by measuring with the same conditions as above but alternating the frequency of deformation between 1, 2, 5, 10, and 30 Hz. The E_a was then calculated by plotting the natural logarithm of the frequency against the reciprocal temperature of the glass transition and using a rearranged form of the Arrhenius equation (Barral et al., 1994; Mahlin et al., 2009):

$$E_a = -R \left[\frac{\partial(ln\, f)}{\partial(1/T_g)} \right]_P \quad (2)$$

where R is the universal gas constant, and f is the frequency of deformation. The E_a of the glass transition is temperature dependent and therefore non-absolute, but determined using the same frequency interval, it can be used to compare systems (Chowdhury and Frazier, 2013).

3.4.2. X-ray scattering

X-ray scattering is a non-invasive technique used to probe fine structural features of materials. It enables the determination of distances between scattering centers, such as atoms or particles, based on their diffraction patterns. Wide-angle X-ray scattering (WAXS) is sensitive to atomic-scale distances in the Ångström range. In contrast, small-angle X-ray scattering (SAXS) examines structural features in the nanometer regime such as interfaces, particles or pores.

WAXS profiles of crystalline materials exhibit sharp, well-defined peaks that can be readily interpreted. In amorphous materials, however, the profiles typically consist of one or a few broad Gaussian-like distributions, the origins of which are either inter- or intramolecular distances. SAXS profiles are sensitive to the size, shape, distribution, and contrast of electron density in nanoscale domains. In many practical systems, SAXS data may exhibit only subtle features, making interpretation challenging. To extract meaningful structural information, modeling is often needed; however, proper interpretation of models requires prior knowledge of the system, such as its composition, morphology, or contrast conditions (Roe, 2000).

One of the main strengths of X-ray scattering lies in its statistical power: it provides rapid, average structural insights over large sample volumes, something that would be time-consuming, or even impossible, with microscopy-based techniques. In this thesis, SAXS and WAXS are used to investigate both lignin and pulp, and how their structures alter upon plasticization.

The peaks and shoulders in the scattering curves can be related to real distance via Bragg's law, $d_{(hkl)} = 2\pi/q_{(hkl)}$ (**eq. 3**), where *hkl* are the Miller indices, which specify the orientation of lattice planes in a crystal. In WAXS, the size of crystalline domains can be estimated via the Scherrer equation, $L_{(hkl)} = 2\pi K/\Delta q_{(hkl)}$ (**eq. 4**), where *K* the Scheerer constant (*K*=1 in this work) and Δq_{hkl} is the line broadening at the half maximum (Garvey et al., 2005). The line broadening at the half maximum was determined by fitting Gaussian functions to the cellulose lattice places of (110), (1-10), (004), and (200) and one peak accounting for amorphous scattering centered at 1.31 $Å^{-1}$. The unordered cellulose, hemicellulose, lignin, and plasticizer all have different amorphous halos; thus, a single gaussian will not be able to accurately account for all the amorphous materials. However, as the (200) signal is so intense, and its narrowing could be visually observed, $L_{(200)}$ was considered possible to determine with some certainty. The crystallinity index (CrI) was estimated using the Segal method (Segal, 1959), **eq. 5**:

$$\mathrm{CrI} = \left(\frac{I_{(200)} - I_{\mathrm{am}}}{I_{(200)}}\right) \quad (5)$$

where I_{200} is the intensity (peak height) for the (200) peak at ~1.59 $Å^{-1}$ and I_{am} the intensity at 1.3 $Å^{-1}$. The $\mathrm{CrI}_{\mathrm{Segal}}$ overestimates the crystallinity of cellulose but can be used comparatively (Salem et al., 2023).

3.4.3. NMR

NMR spectroscopy takes advantage of the nuclear spin of atoms. As a charged particle with a spin will generate a magnetic field, nuclei with non-zero spin, such as ^{1}H, ^{13}C, and ^{31}P appear as small magnets. If a magnetic field is applied (B_0), the spin of the nuclei will orient themselves with or against the field. The energy difference between these two states is related to the bonding environment of the atom (Mirau, 2005).

The energy difference is probed by a radio frequency pulse (creating an oscillating magnetic field) that flips and aligns the magnetization vector (the orientation of spin) of atoms/nuclei. When the magnets are relaxing back to their equilibrium positions, they induce a current in a receiver coil. This signal is a decaying sine wave called the free induction decay. It is decaying as the net magnetization perpendicular to the coil is defocused, i.e. the spins are fanning out. This relaxation is referred to as spin-spin relaxation, as it is governed by energy transfer between nuclei and is associated with the time constant T_2. Another, slower relaxation takes place simultaneously, where the net magnetization vector is moving from perpendicular to parallel with the applied magnetic field. This relaxation is referred to as spin-lattice relaxation and is associated with the time constant T_1 (Mirau, 2005).

The T_1 relaxation time is an important factor in NMR, as it determines the frequency at which scans can be repeated, to achieve a higher signal to noise ratio. ^{1}H nuclei relax quickly, partly due to their high abundance, allowing for faster scanning. In contrast, ^{13}C nuclei relax more slowly, which contributes to longer experiment times.

By using polarization transfer methods, where magnetization is transferred from a fast relaxing to a slow relaxing nucleus, e.g. ^{1}H to ^{13}C, more scans can be collected in a shorter time. Two types of polarization transfer experiments are used in this thesis: cross polarization (CP) and insensitive nuclei enhanced by polarization transfer (INEPT).

In CP, the polarization is transferred by dipolar interactions, whereas INEPT transfers over covalent bonds (J-couplings). CP is used in solid-state NMR (ssNMR) as it is sensitive to rigid molecules but gives no signal for liquid compounds. INEPT, on the other hand, is sensitive to mobile compounds and insensitive to slow-moving molecules (Nowacka et al., 2010).

Polarization transfer can be used to increase the sensitivity of ^{13}C NMR, but as hinted above, it can also be used to study the dynamics and morphology of polymers. CP and INEPT can be used to differentiate rigid and mobile components in a sample (Nowacka et al., 2010), such as plasticizers that have phase-separated from a polymer blend.

It is also possible to study the phase morphology of polymers via spin-diffusion: the transfer of spin to neighboring nuclei by dipolar couplings, i.e. the mechanism active in CP. Proton T_1 ,T_1^H, is influenced by diffusion of spin arising from transfer of magnetization to neighboring protons. The high abundance and strong coupling of protons make spin diffusion a phase-dependent phenomenon; thus, it is possible to differentiate phases based on their relaxation time. In this thesis, the phases of interest are plasticized/unplasticized polymers, cell wall components in the same or different phases, and biphasic relaxation behavior as an expression of morphological heterogeneity.

Within this work, two relaxation experiments were performed: varied spinlock and inversion recovery. In the former experiment the intensity is fitted to an exponential decline (**eq. 6**) and spin-lattice relaxation in the rotating frame ($T_{1\rho}^H$) is calculated, whereas in the latter experiment, the intensity is fitted to an exponential growth and T_1^H is calculated (**eq. 7**). Unlike T_1^H, which describes relaxation back toward alignment with the static field B_0 and is characterized by relaxation times on the order of seconds, $T_{1\rho}^H$ describes the faster relaxation of magnetization aligned with an applied spin-lock field $B_{1,eff}$, with relaxation times on the order of milliseconds. In this thesis, the relaxation time was probed in the carbon domain via CP, enabling

the investigation of the relaxation behavior of all components in the blends. By using mono- or biexponential versions of the equation, the heterogeneity of the phase morphology can be probed.

$$I(t_d) = I_0 e^{-t_d/T_{1\rho}^H} + I'_0 e^{-t_d/T'^H_{1\rho}} \quad (6)$$

$$I(t_d) = I_0(1 - 2e^{-t_d/T_1^H}) + I'_0(1 - 2e^{-t_d/T'^H_1}) \quad (7)$$

where I_0 is the initial (**eq. 6**) or equilibrium (**eq. 7**) signal intensity and t_d is the delay time in the respective experiment, and the apostrophe denotes a second relaxation phase.

Both time constants are associated with an upper limit on the length scale of mixing ($L = \sqrt{6DT_1}$), where D is the spin-diffusion coefficient). In a two-phase system, if the length scale of the individual phase domain is less than L, then a single averaged proton relaxation rate will be measured for both phases, i.e. they are not possible to differentiate. For rigid polymers in the glassy state, L will be about 20 nm and 2 nm for T_1^{H} and $T_{1\rho}^{\mathrm{H}}$, respectively. Thus, by studying both kinds of spin diffusion, the phase morphology can be probed at different length scales (Meurer and Weill, 2008; Mirau, 2005).

4. Inherent properties: the softening of isolated and *in situ* lignins and polysaccharides

4.1. Determining the T_g of isolated lignins

As has often been described in the literature (Clauss et al., 2015; Fox and McDonald, 2010; Souto and Calado, 2022), determining the T_g of lignin using DSC is not always trivial. The change in heat capacity (C_p) over the glass transition for lignin is not large, and as C_p is inversely correlated to molar mass for polymers (Wu et al., 2021), the change becomes even smaller for high-molecular-weight samples. Lignins are also associated with exothermic events close to their T_g and temperatures above, which further obscures the weak endotherm of the glass transition.

Of all the lignins isolated in section 3.1, only the T_g of low-molecular-weight lignins could easily be determined using DSC. All the higher-molar mass lignins either did not exhibit an endothermic event, or it was obscured by an exothermic event (**figure 15a**); however, in the powder sample holder for DMA, the T_g was possible to determine for all lignins of the study (**figure 15b**), and their T_g have been plotted in (**figure 15c**). See **appendix 1** for investigation of the linear viscoelastic region.

Absolute moduli values are unobtainable with the powder sample holder, but relative estimates are possible. All lignins in the glassy state had very similar E' values (**Paper I, figure S1**), but the drop in E' over the glass transition varied. For both the KL fractions (**Paper I, figure 7**) and the isolated lignins (**figure 15b**), the degree of softening (drop in E') correlated with the molar mass, suggesting that flowable lignins are best obtained by chain scissioning. That is, if there is a net reduction in molar mass, even if the lignin also condenses during the treatment, as in kraft pulping, an increased flow in the rubbery state is to be expected. However, the same is not true for the T_g, as we shall see in the next section.

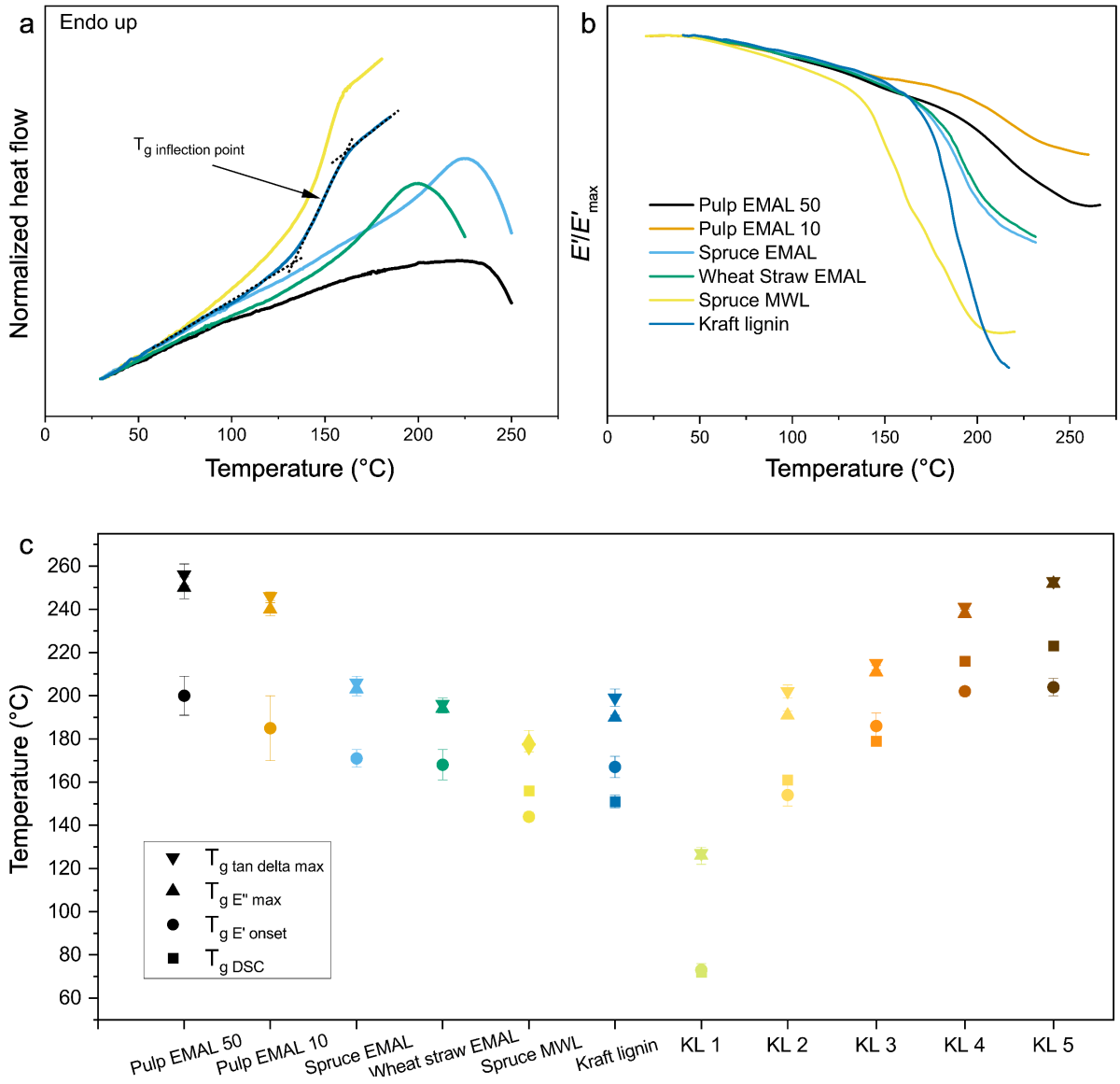

Figure 15. DSC (a) and DMA (b) thermographs of isolated lignins with legend in (b). The T_g of all the lignin in the study determined by both DSC and DMA (c).

4.2. At what temperature do the components of wood and pulp soften and why?

All three major components in wood and pulp – lignin, hemicellulose and cellulose – soften upon heating. The question is when and why these materials soften, a matter which their non-continuous and multilayered organization obscures. The main focus of this thesis is the softening of lignin, but we will here start by looking at the thermal softening of polysaccharides.

Goring (1963) found that cellulose from different sources soften between 230-250 °C, using a plunger tool. He proposed three possible explanations for this softening: the glass transition of the unordered part of cellulose, chemical decomposition or a combination of the two. Later studies have, via molecular dynamics simulations, found that amorphous cellulose has a T_g around 250 °C (Chen et al., 2004; Elf et al., 2023). Likewise, by determining the T_g of plasticized cellulose (cotton linters etc.) and extrapolating to zero plasticizer content, several studies have proposed a T_g of pure celluloses in this region (Paes et al., 2010; Hancock and Zografi, 1994; Szcześniak et al., 2008). A glass transition involves the onset of cooperative movements, something which is difficult to imagine for the unordered surface layer of cellulose (and hemicellulose), but the studies above indicate that the thermal softening of semicrystalline cellulose above 200 °C involves a physical transition akin to a glass transition. However, it remains unclear if chemical degradation also plays a role in the thermal softening observed in holocellulose at these temperatures.

The pseudo-thermodynamic nature of the glass transition can be used to inquire about the nature of the softening – T_g is frequency dependent, whereas softening due to chemical decomposition is not. Thus, by performing a frequency cycling over a temperature ramp, softening due to the two phenomena should be possible to differentiate.

As is evident from **figure 16**, cellulose powder (milled bleached kraft pulp, 97 wt% glycose, see **Paper IV** for details) has a softening event taking place at ~275 °C, but which has no frequency dependency. Isolated softwood GGM, characterized in (Härdelin et al., 2020), on the other hand, has a softening with Arrhenius behavior and an apparent E_a of 1150 kJ/mol, followed by a softening at the same temperature as cellulose. The first is most likely a glass transition whereas the latter could be related to chemical degradation. For cellulose, it is possible that physical and chemical softening coincide. An increased mobility is often also seen to increase thermal degradability, as the increased motion decreases the likelihood of

recombination of heat-severed bonds and allows for greater oxygen diffusion – behavior which has been observed in cellulose derivatives (Tsioptsias, 2021). It is also possible that cellulose has a glass transition unconnected to this degradation, which could not be detected under our conditions. Polysaccharides in wood and pulp appear to contribute to softening in the measured temperature range through both glass transitions and chemical degradation processes.

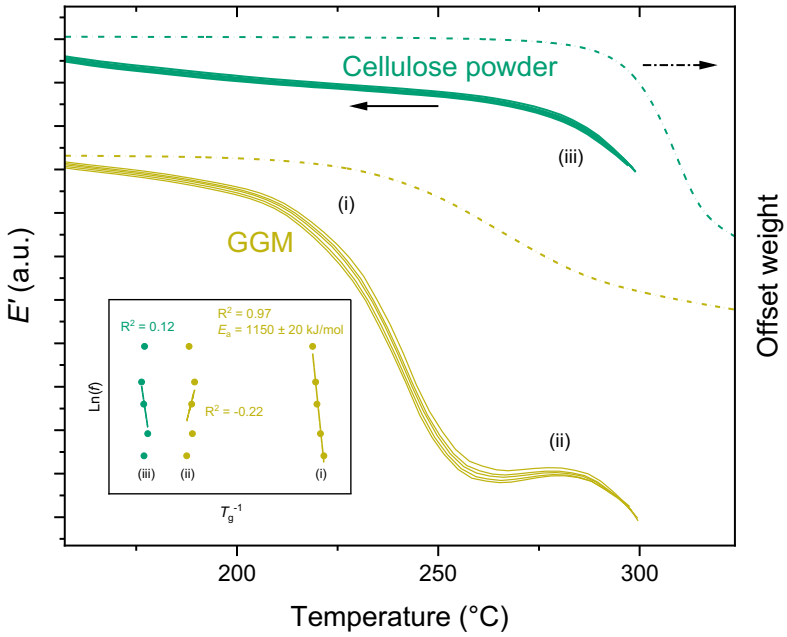

Figure 16. Non-normalized E' as a function of temperature for cellulose powder and a softwood GGM. The GGM composition is described in (Härdelin et al., 2020). The inset shows the inverse of $T_{g\,E'\,onset}$ as a function of the natural logarithm of the frequency of deformation.

Norway spruce, milled to millimeter size (mesh 60) and run in the same DMA set up, has two softening events (**figure 17**): one at 219 ± 12 (here termed T_{low}) and one at 275 ± 8 °C (T_{high}). The latter coincides with the thermal softening of cellulose and the higher temperature softening of GGM, whereas the former would then likely be related to the T_g of hemicellulose or lignin or both. These results are in very good agreement with those of Startsev et al. (2017), who performed DMA on *Pinus sylvestris*, reporting 195 and 277 °C for the corresponding transitions, and providing similar interpretations of their origin.

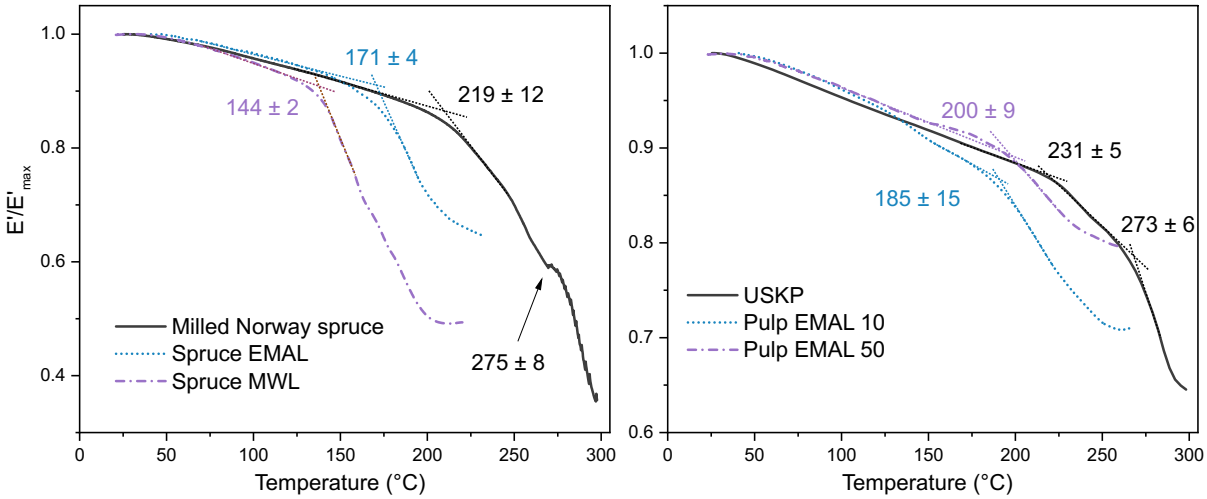

Figure 17. *E'* as a function of temperature for milled Norway spruce (left) and USKP (right) and their respective isolated lignin. Standard deviations are based on 3 and 5 observations for lignins and lignocelluloses, respectively.

With the EMAL protocol, 60 % of the lignin from the Norway spruce was isolated. Its T_g is 171 °C, markedly lower than the softening of spruce, but still closer than that of MWL. Guerra et al. (2006a) and myself (**Paper I**) found MWL and EMAL to have very similar chemical structure, but with EMAL having a much higher molar mass, which explains the discrepancy in T_g. In the Ogawa plot (**figure 18**), which takes better account of the high molar-mass dispersity in the samples than the Fox-Flory, an extrapolated line between the two data points intersects the y-axis at approximately 190 °C. This would mean that spruce lignin at infinite molar mass (**eq. 1**) would be expected to have a T_g around this value, which is consequently closer to what we observe for Norway spruce. The accuracy of this is obviously questionable, as there are only two data points and the molecular-weight determinations are non-absolute, but it nonetheless points towards what others have indicated (Salmén, 1982; Startsev et al., 2017) – that the thermal softening of dry wood at around 200 °C encompasses the glass transition of lignin.

Another concern of this thesis is how the thermoplasticity of lignin fares during kraft pulping. In the past, this has been studied by submerging wood and pulp samples in water or ethylene glycol which shifts the T_g of the holocellulose below zero, and

brings the T_g of lignin down to about 100 °C (Vikström and Nelson, 1980; Heituer and Atack, 1984). The T_g of lignin in pulp and wood can then be compared; however, as is evident in **Paper II**, plasticizers affect different lignins differently – i.e. the plasticization effect of water might be more efficient for the kraft cocked lignin – which would hinder meaningful comparison.

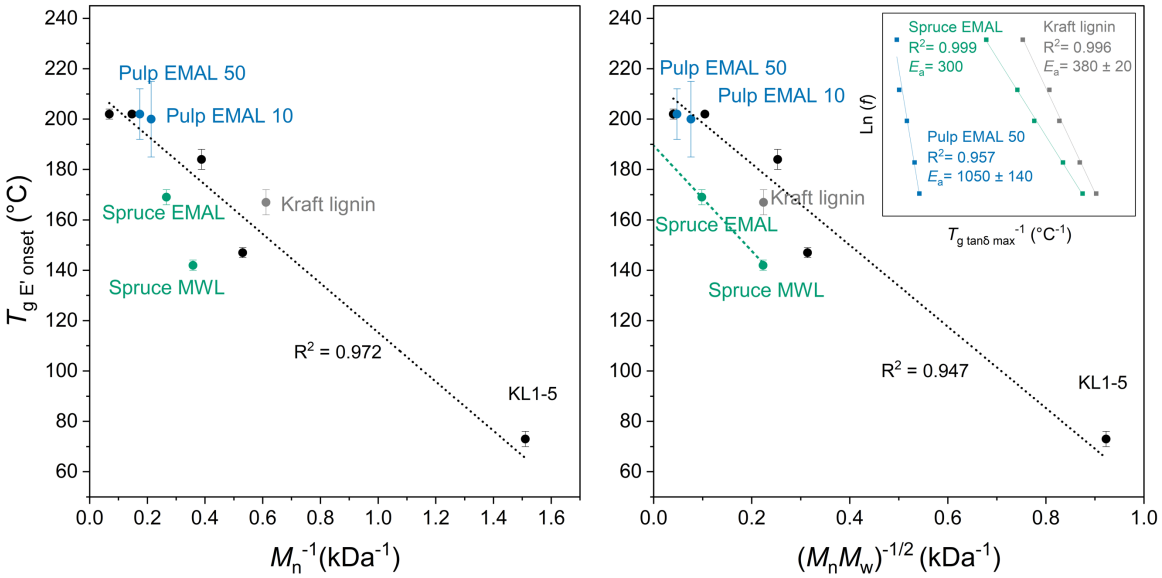

Figure 18. T_g as a function of reciprocal molar mass, M_n (left) and of the $(M_nM_w)^{½}$(right). Kraft lignin (grey), KL fraction 1-5 (black, fitted with a black line), isolated spruce lignin (green, graphically extrapolated line) and Pulp EMAL (blue). Insert in right plot: Arrhenius plot with E_a reported in kJ/mol.

By comparing the first softening (T_{low}) of Norway spruce and unbleached softwood kraft pulp, USKP (**figure 17**), it is evident that USKP softens at a higher temperature. This could be related to loss of hemicelluloses or changes in lignin chemical structure. By isolating the USKP residual lignin with the EMAL protocol, close to half of the lignin was extracted (sample name Pulp EMAL 50). The isolated lignin has a high T_g and a low degree of softening (drop in E'). In the plots in **figure 18**, the T_g of the Pulp EMAL samples falls on the line for kraft lignins, suggesting a comparable restriction of segmental movements. Thus, at a given molar mass, residual kraft pulp lignin would be expected to have a higher T_g than native softwood

lignin. That is, native lignin structures appear to benefit segmental mobility, though the comparatively high molar mass of isolated native and residual lignins mask this.

The softening of Norway spruce and USKP, and their respective isolated lignins, were also investigated with the frequency cycles. The isolated lignins exhibited a clear Arrhenius behavior with E_a in the 300-1100 kJ/mol range (**figure 18** and **table 2**); however, for both Norway spruce and USKP, no correlation with frequency was found for either T_{low} or T_{high}. The reason for not detecting a frequency dependence in USKP and milled wood might be the insensitivity of probing the glass transition in a material with no continuous amorphous phase, or simply that the amorphous polymer content is too low for analysis of such detail. We will return to the question of the T_g of the wood components in, in section 5.2, when USKP is plasticized.

Table 2. E_a of the glass transition based on $T_{g\,E''\,max}$ and the effective $T_{1\rho}^{H}$.

Lignin	$\boldsymbol{E_a}$ (kJ/mol) (n=3)	$\boldsymbol{T_{1\rho\,eff.}^{H}}$ (ms)[c]
Spruce EMAL	300 [a]	7.5 [a]
Softwood kraft lignin	380 ± 20	11.1 ± 0.2 [b]
Pulp EMAL 50	1050 ± 140	9.6 [a]

[a]Single measurement due to lack of material. [b]Duplicated measurement with error calculated as the difference between the values divided by 2.[c]$T_{1\rho\,eff}^{H}$ was calculated as the sum of the population-weighted average of the relaxation rates ($1/T_{1\rho}^{H}$), as we shall see in section 5.1, lignin has heterogeneous spin diffusion.

NMR relaxometry in the rotating frame, $T_{1\rho}^{H}$, was used to probe the phase morphology of the lignins (see next section); however, the $T_{1\rho}^{H}$ values, measured under identical conditions, also allow comparison of molecular dynamics. Although $T_{1\rho}^{H}$ is dominated by spin diffusion and cannot be directly interpreted in terms of correlation times, spin diffusion does depend on molecular mobility (Mirau, 2005). Below T_g, the mobility of lignin is governed by local motions such as ring flips (Kang et al., 2019); therefore, in our samples, $T_{1\rho}^{H}$ is more likely to reflect local chain dynamics. E_a of the glass transition, on the other hand, is a measure of energy barriers for segmental rearrangements (Aharoni, 1972; Ediger, 2000; Chowdhury and Frazier, 2013). Thus, these two parameters probe polymer chain dynamics at different length and time scales. As is evident in **table 2**, E_a follows the molar mass of the lignins, much like the degree of softening (drop in E') over the glass transition did, which is not surprising, as segmental motion and molecular weight are highly correlated below a certain molar mass. However, the $T_{1\rho}^{H}$, probing local motions, appears to be more correlated with the degree of condensation, as Pulp EMAL 50 has an intermediate value. This would suggest that native structures, such as β-O-4, are beneficial for local mobility, whereas condensed structures, such as 5-5', are detrimental.

5. Modified properties: the softening of plasticized lignin and pulp

5.1. Plasticization of isolated native, residual, and technical lignin

In the previous section, we observed that the chemical structure and molar mass significantly influence the viscoelastic properties of lignins. However, it remains unclear whether these structural differences are substantial enough to cause different responses to different types of modifications. In this section, four lignins selected from the original seven lignins isolated in section 3.1, spruce EMAL (SL), wheat straw EMAL (WL), pulp EMAL 50 (PL) and kraft lignin (KL) – chosen for their distinct structural characteristics – will be subjected to different plasticization methods to explore this question (Paper II-III).

Powder DMA was again employed to investigate the plasticized lignins, as they could only be cast into very brittle films, if they formed films at all. Since the 1950s, the standard DMA approach for examining the plasticization of synthetic polymers has involved analyzing mechanical damping profiles (tan δ) and modeling the T_g using more or less complex functions (Nielsen et al., 1950; Bishai et al., 1985; Vilics et al., 1997; Gama et al., 2019). Standard DMA is less commonly applied to isolated lignins, likely due to challenges in producing self-supporting samples and obtaining sufficient quantities of isolated lignin. However, the use of a powder sample holder helps to overcome these limitations.

One aim of this examination was to determine which plasticizer caused the least broadening of the tan δ peak – a measure of the glass transition width. In theory, the plasticizer that distributes most homogeneously within the polymer matrix would result in minimal peak broadening (Mok et al., 2008; Vilics et al., 1997). However, contrary to expectations, a narrowing of the tan δ peak was observed across all lignin-plasticizers blends. An example is shown in **figure 19**, where the normalized tan δ

of plasticized SL is plotted. This unexpected result suggests that, rather than studying the distribution of plasticizers, we are instead observing how the system as a whole is homogenizing. To confirm that this narrowing is not a phenomenon related to measuring powders, an acrylic polymer powder was also plasticized with TA, but here a broadening was instead observed (**appendix 1**). For all lignins except WL, TA is the plasticizer that brings about the narrowest transitions, suggesting good compatibility with many types of lignin structures.

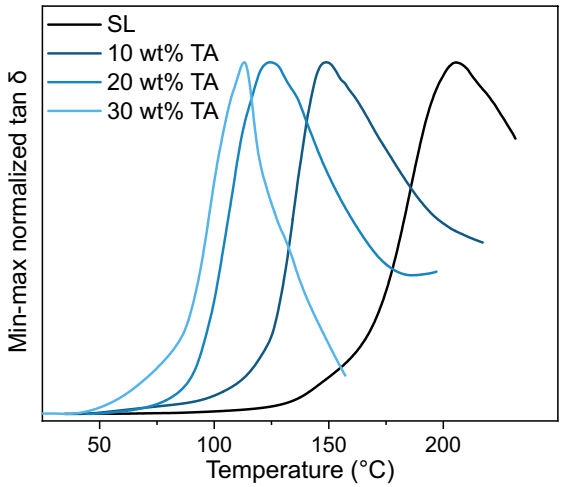

Figure 19. Tan δ for plasticized spruce EMAL (SL) as a function of temperature. The y-axis has been normalized.

The evidence of this homogenization is indirect and there is an uncertainty in using the glass transition to study populations, as the transition is based on cooperative dynamics which are changing with temperature (Cavagna, 2009). To probe the phase morphology directly, the homogeneity of spin diffusion of the two most structurally distinct softwood lignins, SL and KL, was investigated using CP ssNMR relaxometry. Via varied spin lock experiments, the $T_{1\rho}^{H}$ was determined for lignins and TA. TA was used as it produced to greatest narrowing of the glass transition region and is clearly separated from lignin in the ^{13}C spectrum.

Bayesian and Akaike information criterion, which reward low residuals and penalize number of parameters (Brewer et al., 2016), were used to compare the fit of mono or biexponential versions of **eq. 6** (tables with the fitting statistics are find in **Paper III**, **table S4**); however, the better fit is also evident from visual inspection (**figure 20**). Unplasticized SL and KL were found to have a heterogeneous spin diffusion – that is, their relaxation was better fitted with a biexponential – with a rigid majority and a mobile minority phase (**figure 21**). This indicates that there is some heterogeneity in the material with disparate domains larger than a few nm. For KL, for which the relaxation experiment was duplicated on different aliquots (2x~70 mg), the fittings were close to identical.

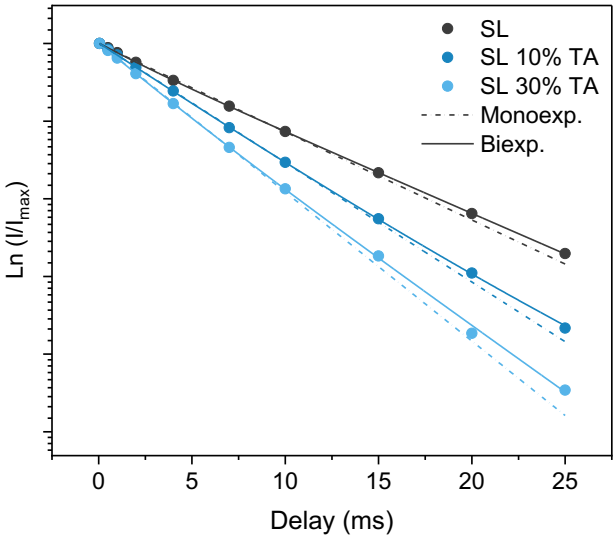

Figure 20. The natural log of max-normalized intensity of lignin-OCH_3 as a function of spin lock time (delay) for spruce EMAL (SL) with and without TA. As evident, the relaxation pattern of the samples is better covered by a biexponential, indicating a heterogeneous chemical environment.

When plasticizer is introduced, the biexponential model continues to provide a superior fit for both lignins, and the distinction between mono- and biexponential fitting criteria becomes increasingly pronounced. At a plasticizer content of 10 wt%, both rigid and mobile phases are still present, showing only minor alterations in their dynamics. The TA appears to have entered both phases, as indicated by the matching $T_{1\rho}^{H}$ values.

At 30 wt% plasticizer, however, the phase morphology changes significantly. In KL, the dominant phase now exhibits a $T_{1\rho}^{H}$ comparable to that of the previously mobile phase, and a new, highly mobile minority phase emerges. This minority phase has grown slightly in size and contains a greater amount of TA. In contrast, SL shows a less dramatic transition: the overall mobility changes less but the two domains become equal in relative abundance, each incorporating a similar proportion of TA.

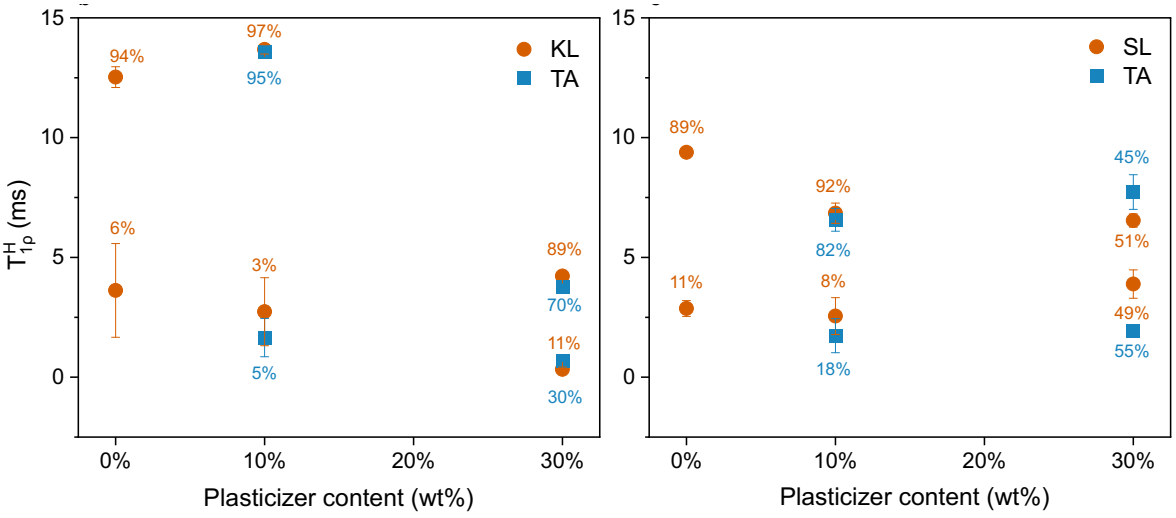

Figure 21. $T_{1\rho}^{H}$ plots for KL (left) and SL (right), where the $T_{1\rho}^{H}$ of the lignins and TA are in orange and blue, respectively. The percentages give the relative abundance of the two phases. See (**Paper III**, **table S4** for fitting statistics and parameters.

With plasticizer, the tendency was for both lignins to have a convergence of the $T_{1\rho}^{H}$ of their two phases. Since both $T_{1\rho}^{H}$ and T_g depend on molecular mobility and interactions, they are expected to be correlated, consistent with reports in the literature (Hill et al., 1999; Liu et al., 1990; Schaefer et al., 1987). Thus, the morphology of these lignins is perhaps not homogenized, as evidenced by their heterogeneous spin-lattice relaxation, but a convergence of the $T_{1\rho}^{H}$ values of the two phases suggests a convergence of local physical properties, such as T_g.

The results above are discussed as two-phased systems, but this one or two-phase dichotomy is forced on the samples by modeling spin-lattice relaxation as a mono- or biexponential. There is no evidence in DSC or DMA for a two-phase polymer

system. Two other possibilities, not based on phase separation, are that gradients in the chemical environment exist within the material, with certain lignin structures aggregating into something less well defined than a phase – akin to gradient copolymers (Mok et al., 2008). The other explanation is the inherent spatial heterogeneity of glass-forming materials. Below T_g, cooperatively rearranging regions develop independently, causing even single-component liquids to exhibit local variations in dynamics (Ediger, 2000). It could also be a combination of the two: the inherent spatial heterogeneity of glasses is further enhanced by the compositional heterogeneity of lignin. Nonetheless, the physical properties of these local gradients appear to homogenize.

At 10 wt% plasticizer content, the T_g-depression is relatively uniform for all the plasticizers-lignin combinations (**figure 22**). It is only at higher plasticizer concentrations that the curves start deviating, with some plasticizer-blends starting to plateau. Such behavior would suggest that the plasticizer has phase separated, and indeed, in both DSC and INEPT, these samples do exhibit a liquid plasticizer phase (**Paper III**, **table 3**). As discussed in **Paper II**, the solubility of plasticizers in different lignins could only be partly predicted using Hansen solubility parameters (HSP).

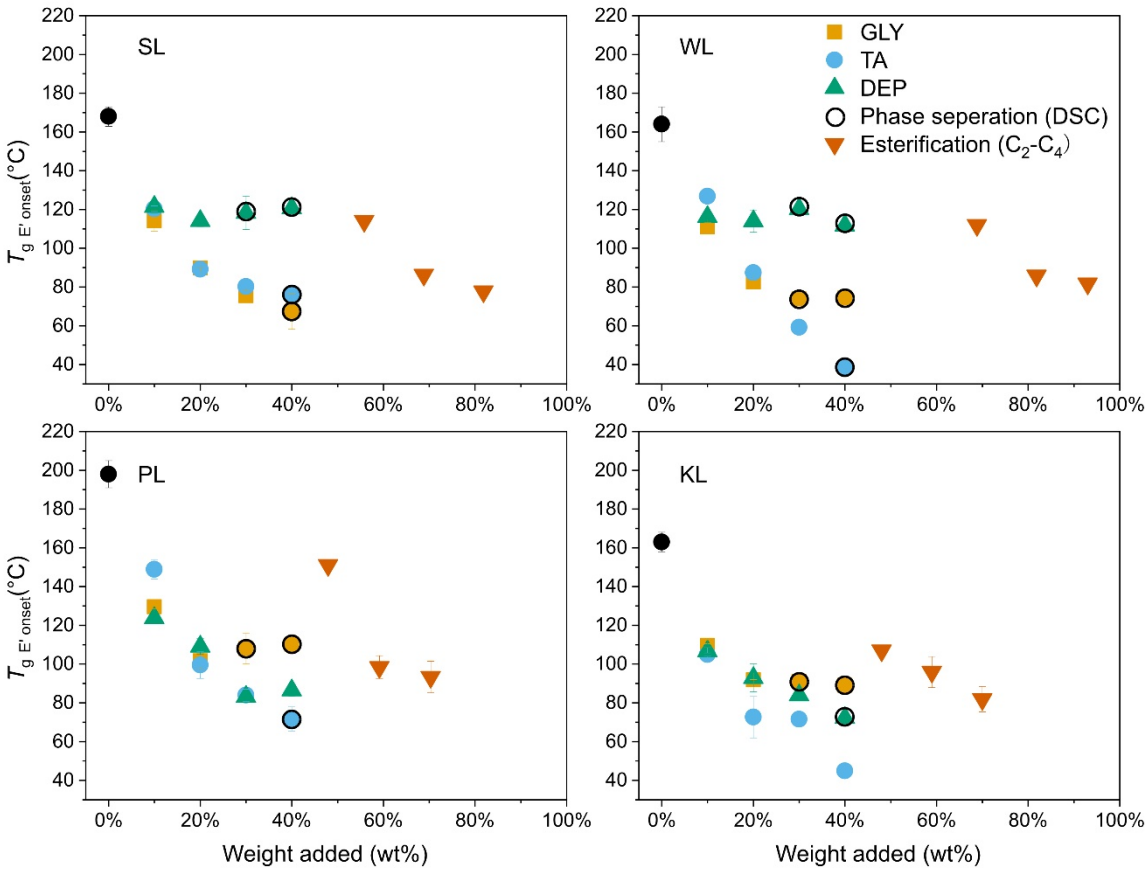

Figure 22. T_g determined as the onset of E' as a function of plasticizer content or weight increase upon esterification.

The lignins were also quantitatively esterified to compare their efficiency to external plasticization. Esterification was found to be much less efficient in reducing the T_g of lignins on a weight-addition basis. This has been observed for synthetic polymers as well and, via molecular dynamics simulations, it was suggested to be due to the lower dynamics of a covalently attached side chain compared to a small plasticizer molecule (Klähn et al., 2019). It is interesting to note that the narrowing of the glass transition was not observed upon esterification, suggesting that it is a solubilization effect that homogenizes the properties of lignins (**Paper II**, **figure 3**).

The uniform T_g at 10 wt% plasticization, would suggest that no superior organization arises from any specific combination of lignin and plasticizer. However, this is slightly misleading, as the plasticizers have different molar mass. On a molar basis, TA and DEP are twice as effective as GLY at reducing the T_g. This discrepancy in molar performance suggests that there are specific plasticizer-lignin interactions involved. Lignins have high cohesive energy and to achieve chain spacing and mobility, strong lignin-lignin interactions must be overcome. Thus, one of the aims of plasticization is to disrupt these interactions. Hydrogen bonding in lignin, both inter and intramolecular, governs much of lignin mobility and conformation (Elf et al., 2025; Petridis and Smith, 2016; Vural et al., 2018a). Aprotic plasticizers such as TA and DEP can only accept hydrogen bonding, whereas GLY can both accept and donate. This means that GLY could form hydrogen bonded bridges between lignin molecules, restricting chain movement, as has previously been observed for both synthetic and biopolymers with similar plasticizers (Song and Wang, 2020; Stukalin et al., 2010; Özeren et al., 2020). Such bridges are much less likely with aprotic plasticizers.

To probe the mobility of the lignins at room temperature, CP NMR was again utilized. As CP becomes less efficient with increasing molecular mobility, signal intensity can be used to probe dynamics. The intensity of lignin resonance as a function of contact time, i.e. the time that polarization is transferred from ^{1}H to ^{13}C, is seen in **figure 23**. From this plot, it is evident that plasticization increases the mobility of lignin, as all plasticized samples have a lower intensity than the respective untreated lignin. Likewise, the aprotic plasticizer, TA and DEP, lower the intensity to a greater extent than GLY does. This would then suggest that the hydrogen bonding potential of GLY is antagonistic to lignin mobility.

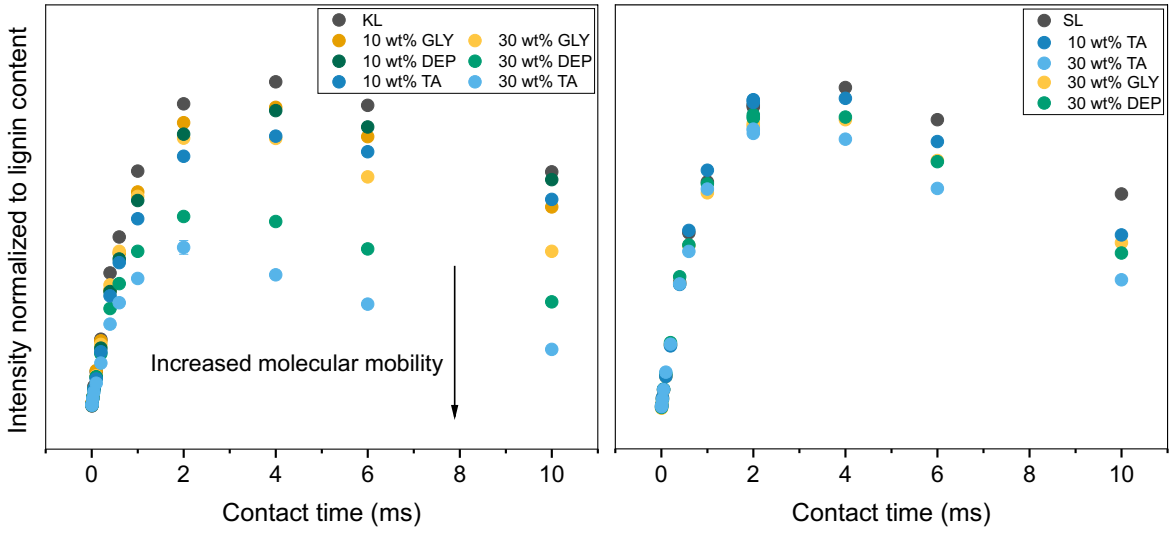

Figure 23. CP-build up and decay of O-substituted aromatic carbon resonance as a function of contact time of plasticized kraft lignin (left) and spruce lignin (right). Adopted from **Paper III**.

5.2. Plasticization of pulp: interactions and thermal deformation

In this section, how plasticizers distribute themselves in the pulp cell wall and if softening of the amorphous matrix changes deformation mechanisms will be investigated. The unbleached softwood kraft pulp of this thesis, USKP, was plasticized with TA and GLY via water submergence and subjected to spectroscopic investigation. The amount of plasticizer in the pulp materials was quantified via Soxhlet extraction and was found to be around 2, 5 and 15 wt% (the materials are named USKP-wt%-plasticizer. See **Paper IV**, **table 1** for details). The plasticized pulp was then hot pressed, and the reorganization of the cell wall was examined with WAXS and SAXS. GLY and TA were chosen as they were expected to lead to selective plasticization, partly based on the high affinity of TA for lignin (**Paper II** and **III**) and its immiscibility with amorphous cellulose (Elf, 2025), and the relatively high affinity of GLY for all cell wall components, found in both molecular dynamics simulations (Elf, 2025) and HSP (Hansen, 2000; Ni et al., 2016; Sun and Sun, 2024). This hypothesized selectivity could then be used to further inform on the role of plasticizers on thermal deformation.

The first question to answer is if the plasticizer has transversed the entire cell wall (i.e. from outer surface to lumen) and if the plasticizer is molecularly dispersed in the cell wall or exists as a liquid phase. By performing line-scans of cross sections using optical photothermal IR (O-PTIR), a confocal IR spectroscopic technique, the impregnation could be studied with a 500 nm spatial resolution (i.e. ~6-13 points of analysis per cell wall) (**figure 24**). In all TA-containing fibers analyzed, TA was found in all sites of analysis, indicating that 48 hours was sufficient time for impregnation; however, the distribution was very uneven. GLY was not possible to differentiate from the polysaccharides using O-PTIR, but there is no reason to assume that its micro-scale distribution would look much different.

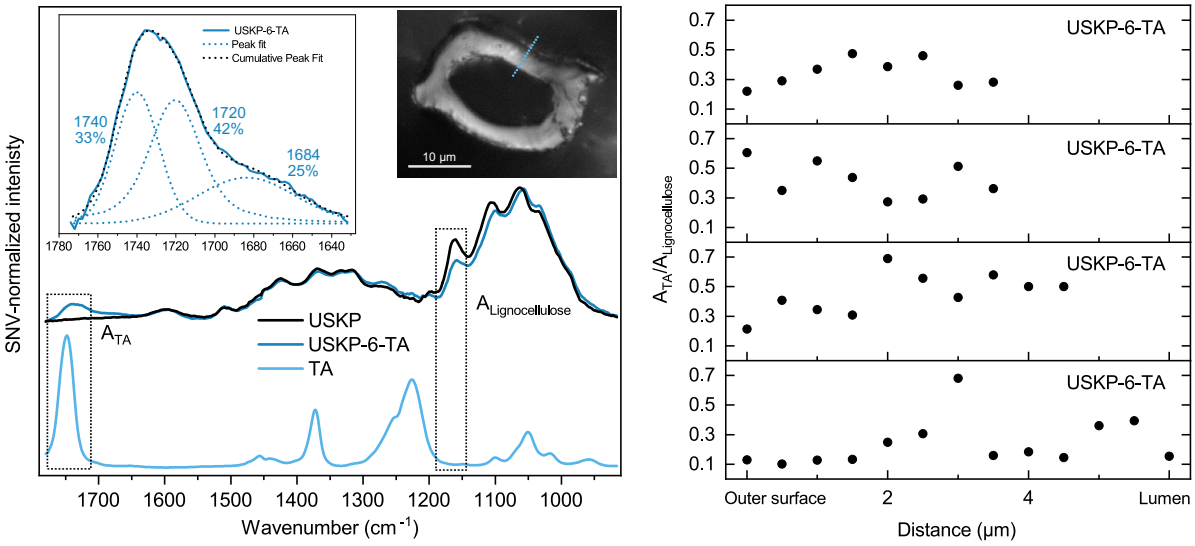

Figure 24. Average of all USKP-6-TA and USKP spectra normalized to standard normal variate (SNV) (left), with inset with the difference spectrum between USKP-6-TA and USKP, fitted with three Voigt functions (pure TA is centered at 1748 cm^{-1}). Line scans of USKP-6-TA fiber cross sections plotted as the ratio of carbonyl stretching (1765-1710 cm^{-1}) to the vibrational band of lignocellulose (1180-1140 cm^{-1}) as a distance from the outer surface (left).

As TA is aprotic, it does not engage in hydrogen bonding in its pure state; but upon addition to the hydroxyl-rich environments of pulp, hydrogen bonding would be expected. The carbonyl-stretching peak (1800-1650 cm^{-1}) shifts to lower wavenumbers when hydrogen is being accepted (Oram et al., 2020), which was also observed for the pulp samples. Upon plasticizing pure cellulose powder, and the

lignin isolated form the pulp, PL, similar redshifts were observed; however, the shift was slightly larger for PL – most likely due to interactions with the more acidic phenol OH groups (**Paper IV**, **figure S4**). A rough estimation of TA interacting with either holocellulose or lignin in the pulp, calculated based on the integrated carbonyl peaks of the plasticized pure compounds, suggests that a majority of the TA (~70 %) is interacting with the holocellulose.

Several ssNMR experiments were performed to further investigate the pulp and the distribution and interactions of the plasticizers. By conducting both CP and INEPT, plasticizers behaving as either solids or liquids could be differentiated. The CP spectra in **figure 25a-b** partly confirm the O-PTIR findings: a majority of the TA is behaving like a solid, molecularly dispersed in the cell wall (assignment of the cell wall components in **figure 25d**). However, a minority part has the dynamics of a liquid, as evidenced by TA resonance in the INEPT spectra, indicating that it is phase separated. GLY only resonated in CP, indicating its total molecular dispersion in the cell wall, most likely due to its higher affinity for polysaccharides.

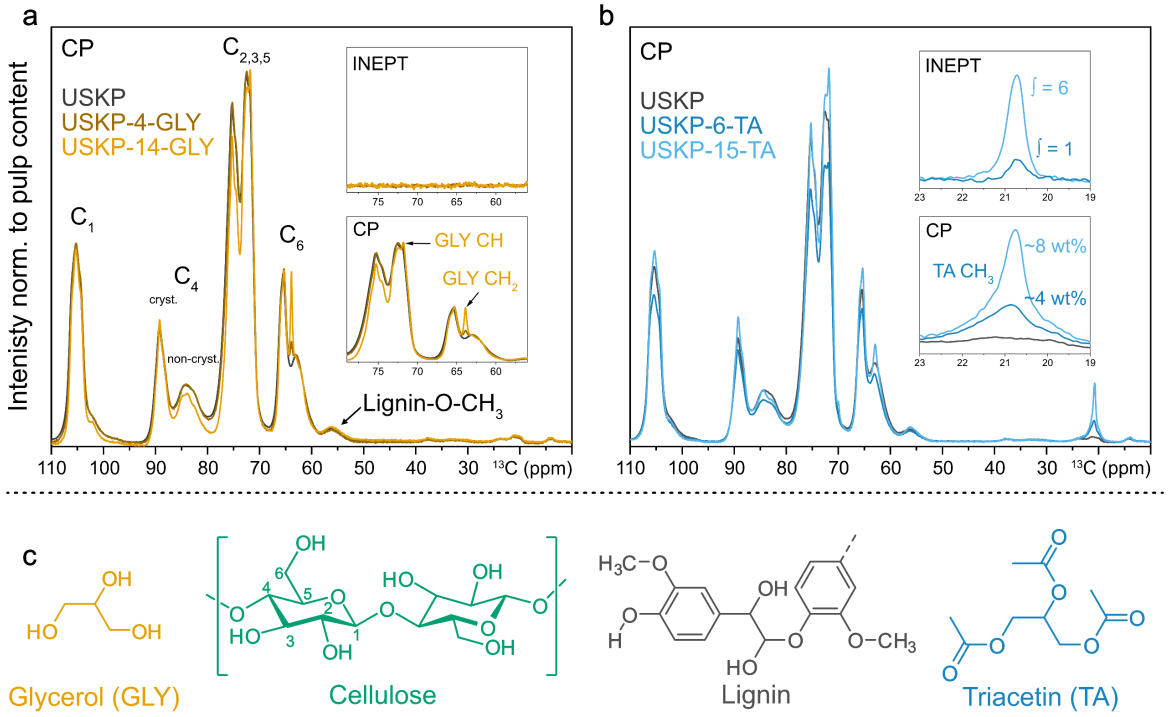

Figure 25. CP spectra with CP and INEPT insets of the plasticizer region (a & b). In (b), the relative amount of TA in CP has been quantified. Structure and color coding of plasticizers, cellulose and part of lignin (c).

Relaxometry ssNMR was used to investigate changes in the chemical environments of the cell wall components of USKP. As the carbon spectrum of GLY overlaps with the polysaccharides, the following ssNMR experiments will only be conducted on TA-containing pulp. The integrals of $C_{4\ cryst.}$, $C_{4\ non\text{-}cryst.}$ and of the OCH_3 of lignin all have relaxation patterns (in both T_1^H and $T_{1\rho}^H$) best fitted with a monoexponential, indicating single phases (**figure 26**. Fitted data and fitting statistics in **Paper IV**, **figure S2** and **table S2**). The only exception was $T_{1\rho}^H$ for $C_{4\ non\text{-}cryst}$, which is better fitted with a biexponential – perhaps due to the inclusion of hemicelluloses in the integral range (see **Paper IV** for full experimental detail). The matching T_1^H of $C_{4\ cryst.}$ and $C_{4\ non\text{-}cryst}$ and the different value for lignin suggest that the polysaccharides and lignin occupy distinct domains in the ~20 nm range, indicating that larger lignin domains remain after pulping.

Both T_1^H and $T_{1\rho}^H$ relaxation changed upon plasticization. All carbons were now better fitted with a longer single T_1^H, indicating a changed chemical environment. In $T_{1\rho}^H$, the polysaccharides appear to be partly plasticized by TA with a majority populations remaining more or less unchanged, whereas the entire lignin population appears to change. The new $T_{1\rho}^H$ matches those of TA (also biexponential decay), further indicating their molecular mixing. T_1^H relaxations find that the entire populations of the fitted carbons have changed, whereas $T_{1\rho}^H$ relaxations indicate a partial plasticization. The reason for this is likely the slower relaxation of T_1^H, which homogenizes local differences.

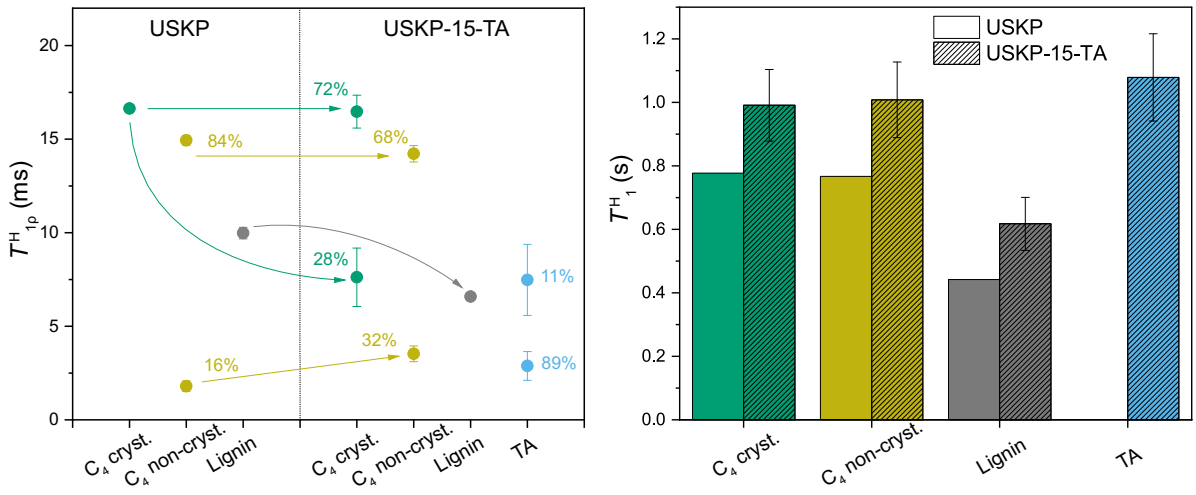

Figure 26. $T_{1\rho}^H$ (left) and T_1^H (right) of USKP with and without 15% TA. The percentages of the phases are their relative abundances (I_n/I_{tot}) and should be considered semi-quantitative.

It would appear as if water-mediated plasticizer impregnation can be performed to introduce plasticizers into the entire cell wall of pulp, even if the absolute amount appears to vary greatly. TA and GLY were chosen with the aim of achieving selective plasticization (lignin and lignin-holocellulose, respectively). As TA was found to interact with all components (no direct TA-hemicellulose interaction was detected, but cellulose is unlikely to be plasticized without the hemicelluloses), this aim does not appear to have been achieved, at least not in a qualitative manner. But perhaps quantitatively, as the change in $T_{1\rho}^H$ was only partial for the polysaccharides and parts of the TA was phase separated.

To investigate the thermal transitions of the plasticized pulp, the powder sample holder for DMA was again used. Upon plasticiation, T_{low} shifts to lower values, whereas T_{high} remains (**figure 27**), which further strengthens the case for T_{high} being related to degradation and T_{low} the glass transition of lignin. In most replicates of the pulp containing ~15 wt% plasticized, a single T_{low} was found around 120 °C, but for 2 and 5 wt%, there was tendency for two drops in E' in the 100-200 °C range (**Paper IV**, **figure S7**), possibly due to the uneven spread of the plasticizers.

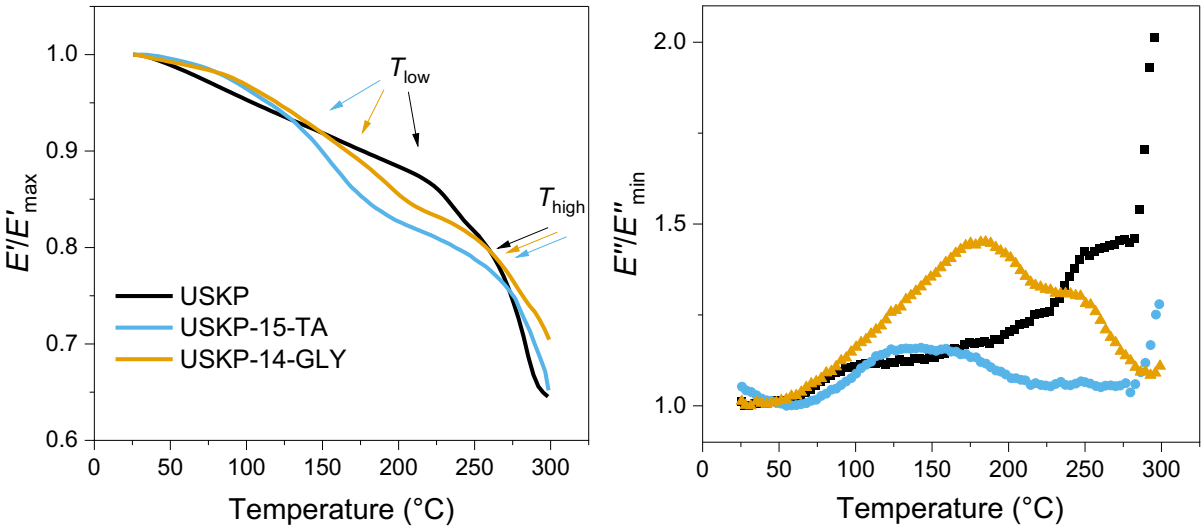

Figure 27. E' (left) and E'' (right) as a function of temperature of USKP with and without plasticizer.

To investigate the plasticizers effect on the thermomechanical induced deformation on the fiber cell wall, USKP with and without 15 wt% plasticizer was hot pressed below and above T_{low}, the supposed T_g of lignin, and subjected to WAXS and SAXS analysis. The hot-pressing was triplicated, and all samples were measured. The scatter profiles displayed below are averages of these, but the calculated parameters are based on the three individual measurements.

Adding plasticizers to both wood and pulp leads to changes in the scattering plots of WAXS. The amorphous halo of the plasticizers, just as the halos of hemicelluloses and lignin, complicates the interpretation of the crystalline peaks of cellulose. The halo of both TA and GLY center at around 1.3 $Å^{-1}$(**Paper IV**, **figure S8**), contributes more to the broad crystalline peaks of cellulose than an amorphous background, which is the reason for the apparent increase in CrI (**figure 28**). The higher $L_{(200)}$ for plasticized USKP is likely due to them retaining a more swollen system, as drying of pulp typically reduces $L_{(200)}$ due to drying-induced distortions of the crystal structure (Paajanen et al., 2022).

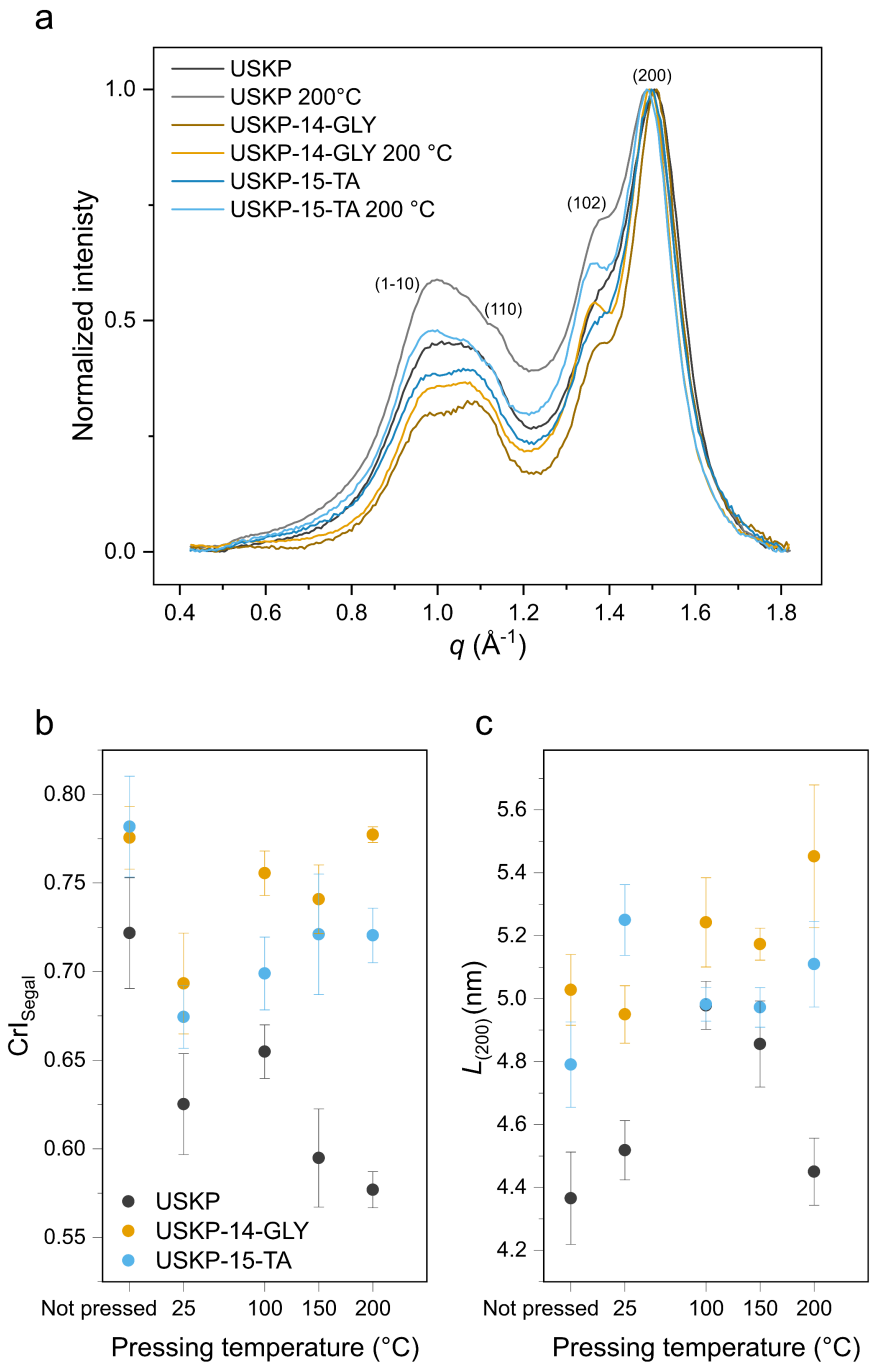

Figure 28. WAXS scatter plots of pulp with and without plasticizer, not pressed or pressed at 200 °C (a) and CrI_{Segal} (b) and $L_{(200)}$ as a function of pressing temperature (c). No shifts in the $q_{(200)}$ position are statistically significant.

Hot-pressing untreated USKP with a pressure of 330 MPa reduced the CrI, with lower values observed at higher temperatures. Cellulosic materials exhibit increased crystallinity under compression at lower pressures (5-200 MPa) (Kumar and Kothari, 1999; Vaca-Medina et al., 2013; Ek et al., 1995), which at pressures around ~250 MPa then fall below the original crystallinity (Ek et al., 1995; Pintiaux et al., 2019; Gravitis et al., 1991). Pintiaux et al. (2019) proposed that friction between cellulose elements under heavy pressing generates enough heat to disrupt crystal structures and cause depolymerization. It appears that the cellulose in the pressed USKP has undergone similar amorphization.

Upon pressing the plasticized samples no, or only very minor, change in crystallinity was observed (ANOVA in **Paper IV**, **table S3**). The exceptions were samples pressed at 25 °C and, for UKSP-15-TA, also at 100 °C, where CrI is reduced. This would indicate that the plasticizers help preserve the cellulose structure under high pressure, at least when operating at or above the T_g of lignin. The preservation of cellulose crystallinity would then be the result of the yielding of the lignin matrix, as well as by the lower cohesion between MF or MF bundles or both, allowing for displacement of cellulose elements, rather than fracture. The same trend in crystallinity was observed for a subset of samples analyzed with CP ssNMR (**Paper IV**, **figure S3**).

Close to all samples exhibit narrowing of the cellulose lattice plane (200) upon hot-pressing, which via the Scheerer equation is interpreted as an increase in $L_{(200)}$. This increase could be due to MF aggregation as (200) is transverse to the MF axis, but also the result from stress-induced lattice distortions. On reducing the crystallinity of cellulose with ball milling, $L_{(200)}$ is also seen to decrease (Ling et al., 2019; Avolio et al., 2012); however, this is not necessarily the case upon compression, which promotes chain packing. It is possible that, in the case of USKP, the fewer remaining crystals have grown in lateral size. For plasticized samples, the same lateral growth is possible, but with less disruption of MF crystallinity to achieve it. The

reorganization of the cell wall and possible aggregation of cellulose will be further analyzed with SAXS.

The SAXS data were initially considered to be modeled with the WOODSAS model, with or without the extra form factor for randomly oriented MF (Hashimoto et al., 1994; Penttila et al., 2019); however, the scattering of untreated or processed USKP could not be fitted with either, thus, we've had to resort to more qualitative assessments. A common approach to analyzing the scattering curves of wood and pulp is to construct Kratky plots (**figure 29**, for log-log plots, see **Paper IV**, **figure 9**), where the peak centered around 0.2 $Å^{-1}$ has been interpreted as containing both MF cross-sectional and lateral packing information (Björn, 2025; Virtanen et al., 2015; Brännvall et al., 2021; Testova et al., 2014).

Paper in the wet state, or with plasticizers, has this peak shifted to lower *q*, suggesting swelling of the system (Björn, 2025; Eliasson, 2025). With GLY, the same shift occurs in our samples (**figure 29**). With TA, the peak at 0.2 $Å^{-1}$ is lost, and a shoulder instead appears at around 0.05 $Å^{-1}$ (~13 nm in real space), possibly corresponding to the scattering of phase separated TA.

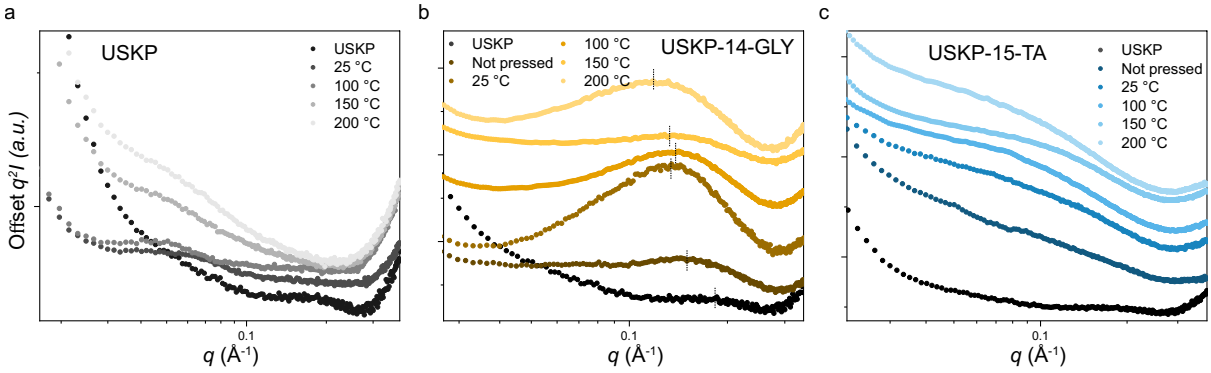

Figure 29. SAXS scatter displayed as Kratky plots of USKP (a), USKP-14-GLY (b), and USKP-15-TA (c). The lines in (b) are fitted graphically.

Upon pressing USKP, at both low and elevated temperatures, the 0.2 $Å^{-1}$ shoulder disappears and a shoulder around 0.05 $Å^{-1}$ becomes apparent. In wood, the shoulder appearing in this region has been ascribed to MF bundles (Penttilä et al., 2020; Penttila et al., 2019), perhaps indicating increased scattering of MF bundles due to densification and aggregation upon pressing, which obscures scattering from smaller features.

Hot-pressed USKP-15-TA and USKP-14-GLY, has their respective features shifted to lower q – peaks clearly shifting from 4 to 5 nm in the case of GLY and shoulders with a less pronounced shift (around 12 nm) for TA – indicating the formation of larger aggregates. Another feature, unique to the plasticized samples, is a shoulder appearing at the very low-q end in the log-log plots, which also suggest aggregation, but in the 50 nm range.

The interpretation of these results is not univocal; however, the SAXS data clearly indicates a change in the organization of the cell wall, possibly involving aggregation. The increase in $L_{(200)}$ can therefore be more confidently attributed to a growth in crystal size.

6. Conclusion and future remarks

The molecular stiffness of isolated native, residual and technical softwood lignins was evaluated by several means. When it comes to segmental chain mobility, molar mass appeared to play a greater role than chemical structure, with PL having the smallest change in E' over the glass transition and the highest apparent E_a of the glass transition. Fox-Flory and Ogawa plots were used to allow comparison beyond the effect of molar mass. KL and PL appeared to have a more similar relationship between molar mass and T_g than SL. Thus, native structures appeared to be beneficial for this larger-scale mobility. For local mobility, as evidenced by $T_{1\rho}^{H}$, PL was found to be intermediate between KL and SL, likely relating to its intermediate chemical structure. This would suggest that native, or less condensed structures, are also beneficial for allowing local dynamics. In a recent molecular dynamics simulation study on lignin dimers (Hackenstrass et al., 2024), β-O-4 linkages exhibited a uniquely high degree of conformational freedom, which could likely translate into higher dynamics at both local and segmental scales.

Even though the Fox-Flory and Ogawa plots were not fully satisfactory, in terms of narrow dispersity, molar mass fractions for all included lignins and absolute molar mass, they still gave insights, and the first hypothesis is not rejected. But it does open for future investigations, such as fractionating EMALs into molar-mass groups, and constructing more reliable Fox-Flory plots, from which the actual $T_{g,\infty}$ could be determined. Compared to the softening of *in situ* lignin, these values could give insights into how the physiochemical environment in the cell wall affects lignin (LCC, confinement etc.).

External plasticization was found to be a more resource-efficient route for lowering the T_g and enabling flow of lignins, compared to esterification, for all lignins in the study. Solubility of the plasticizer in the given lignin was more important than specific plasticizer-lignin interactions; however, the aprotic and flexible TA was

highly compatible with all lignins, enabling higher dynamics in both the glassy and rubbery state. The second hypothesis was therefore not rejected but accepted with a caveat: there are specific lignin-plasticizer compatibilities, but some plasticizers are more universally compatible than others.

Plasticization was also found to increase homogeneity of physical properties, suggesting that fractionation is not the only route for circumventing heterogeneity. However, plasticization of all the various lignins in this thesis only produced brittle powders or viscous pastes, indicating that plasticization is not sufficient for materials where lignin is the matrix component; however, in the cell wall, where lignin is locked into a cellulose network, this would be less of an issue.

Spectroscopic investigations of water-mediated impregnation of lignin-containing pulp with GLY and TA, found molecular dispersion of the plasticizers within the cell wall, and, for TA, complete distribution across the cell wall. GLY appeared to have a greater affinity for the pulp material, with no phase separation detected, whereas TA was less compatible; however, both O-PTIR and ssNMR indicated that TA is indeed in contact with all the major components of the cell wall: holocellulose and lignin.

DMA detected two reproducible softening temperatures in both milled Norway spruce and the pulp, where the higher (275 °C) was ascribed to the degradation of holocellulose. The lower softening temperature, 219 °C for spruce and 231 °C for the pulp, are likely associated with the T_g of lignin, partly due to the higher temperature in the pulp (in accordance with the investigation of their respective isolated lignin), but also due to its shift down to ~120 °C upon plasticization of the pulp, which is commonly observed for *in situ*, plasticizer-submerged lignin.

Pressing the pulp at high pressure was found to destroy the crystalline structures of cellulose, except in the presence of plasticizers and at temperatures around or above the T_g of lignin. The maintained crystallinity suggests that plasticized pulp is deformed with less friction and fracture in the fiber wall, especially when lignin is

softened. GLY appears to preserve the structure better than TA, especially at lower temperatures. Since GLY is expected to act as a more effective plasticizer for the holocellulose content – based on HSP, molecular dynamics simulations, and the greater phase separation observed for TA – the improved preservation may be attributed to reduced cohesion between GLY-plasticized holocellulose elements. Our results, even if not completely proving the third hypothesis, that plasticization of the lignin phase facilitates a more plastic displacement of cellulose elements, are in line with its consequences.

The role of lignin in deforming the cell wall plastically is not completely elucidated. Temperature dependence suggests that lignins need to soften for the observed effect, but thermal softening of the polysaccharide constituents could, even if it was not observable in DMA, also play a role. Another subject of great interest is the *in situ* investigation of the glass transition of lignin and polysaccharides. The INEPT-CP ssNMR tandem which proved effective in this thesis, has previously been proposed as a powerful spectroscopic approach for studying glass transitions (Nowacka et al., 2010). This method could be further utilized to univocally identify which components contribute to the softening behavior observed in DMA measurements.

7. Acknowledgments

I would like to thank my supervisor Anette Larsson for her support, guidance, and for her ability to question everything I do without ever saying *no*. I would also like to thank my co-supervisors Ulrica Edlund and Gunnar Westman for aiding me with their competence in this endeavor and my examiner Merima Hasani for support on both wood chemistry and Chalmers formula.

I would like to thank my two first supervisors, Yvonne Fors and Charlotte Björdal, who first introduced me to the field of wood science through my bachelor's and master's theses on archaeological wood – which, if one is superficial, is mostly lignin.

I would like to thank the students whose theses I had the pleasure of supervising – Rattanapon Tansatien, Vera Svennberg, and Louise Wilson – for fun and, hopefully, mutually instructive projects. I also want to thank lab assistants Herman Miller and Hampus Johansson for their valuable work in the laboratory.

I would like to thank all my collaborators and coauthors. Especially Tobias Sparrman at the NMR-center at UMU for introducing me to the solid-state side of NMR and Linnea Björn for taking the time to direct me in the reciprocal world of scattering X-rays. I would also want to thank Alexandar Matic and Ezio Zanghellini for cheerfully allowing me into the well-maintained and well-equipped labs of Materials Physics.

I would like to thank my fellow doctoral candidates and doctors in Anette's group, both former and current members, for support and help. The same thankfulness is extended to the research groups of Anna Ström and Merima Hasani.

I would like to thank the Chalmers library for its excellent service – I cherish all the obscure documents you have been able to track down for me during these past four years.

Lastly, I would like to thank my husband, Benoit Maire, for his contributions, graphical and familial.

This research was funded by *FibRe* - a Vinnova-funded Competence Centre for Design for Circularity: Lignocellulose based Thermoplastics (2019-00047).

Appendix 1. Method validation: powder sample holder for DMA

At a lignin loading of 30 mg, the powder pocket reached a strain of 15 μm before the instrument's maximum force limit of 18 N was exceeded. To evaluate whether these amplitudes fell within the linear viscoelastic region, kraft lignin (KL) was subjected to an amplitude sweep at room temperature at a frequency of 1 Hz. The sweep was performed twice, and the resulting curves are shown in **figure A1**. The identical responses in both repetitions indicate that the material behaved within the linear viscoelastic range.

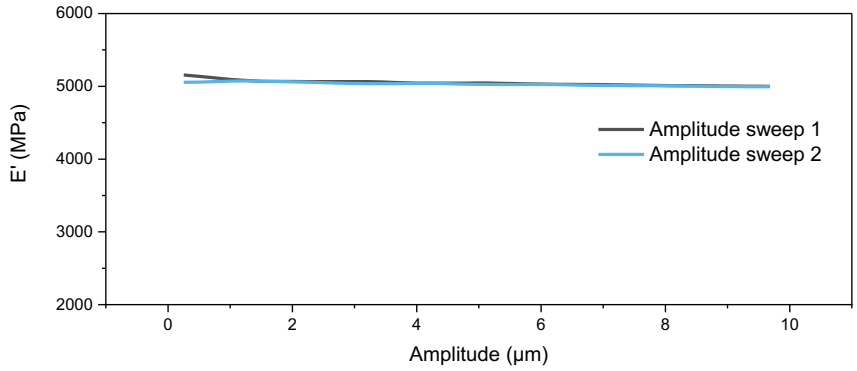

Figure A1. Amplitude sweeps of kraft lignin at room temperature.

To evaluate if glass transition regions broaden in the powder sample holder for DMA due to friction between particles, a commercial poly(methyl methacrylate) (PMMA) was run both as a powder in the pocket and as a hot-pressed film in tension mode (**figure A2**). There was no significant broadening between PMMA measured as a film or as a powder, but upon plasticization with 10 wt% TA (added with the same procedure as for plasticization of lignin), there is a slight increase in broadening, especially at onset.

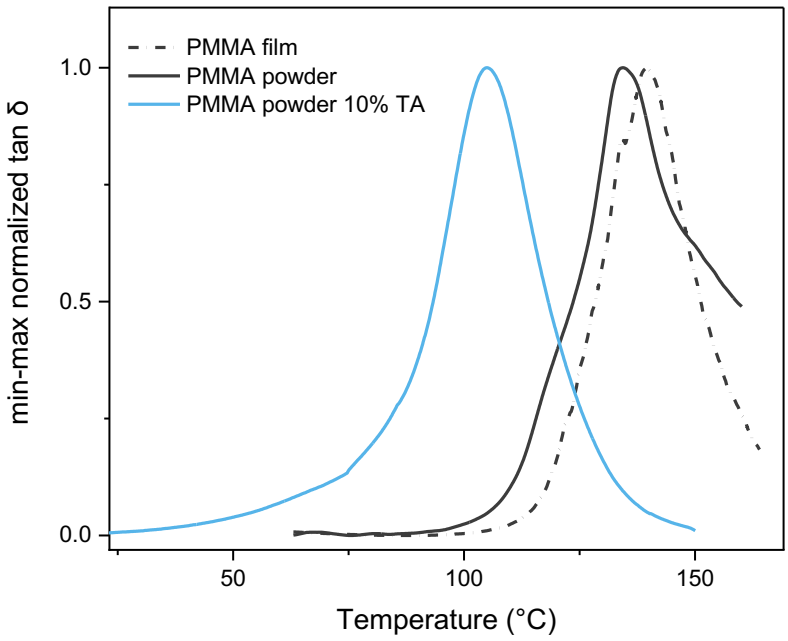

Figure A2. Tan δ as a function of temperature of PMMA run as a film (tension) and as a powder (powder sample holder) and as a powder plasticized with 10 wt% triacetin (TA).

8. References

Adam G and Gibbs JH (1965) On the Temperature Dependence of Cooperative Relaxation Properties in Glass-Forming Liquids. *The Journal of Chemical Physics* 43(1): 139-146.

Afshariantorghabeh S (2024) *Thermoforming of fibre-based materials: an investigation into material characteristics and process variables*. PhD thesis, Lappeenranta-Lahti University of Technology, Lappeenranta.

Aharoni SM (1972) Ductile and brittle behavior of amorphous polymers. Relationship with activation energy for glass transition and mechanical fracture. *Journal of Applied Polymer Science* 16(12): 3275-3284.

Argyropoulos D, Sun Y and Palus E (2002) Isolation of residual kraft lignin in high yield and purity. *TAPPI Journal* 28(2): 50-54.

Asikkala J, Tamminen T and Argyropoulos DS (2012) Accurate and Reproducible Determination of Lignin Molar Mass by Acetobromination. *Journal of Agricultural and Food Chemistry* 60(36): 8968-8973.

Avolio R, Bonadies I, Capitani D, et al. (2012) A multitechnique approach to assess the effect of ball milling on cellulose. *Carbohydrate Polymers* 87(1): 265-273.

Ayoub A, Treasure T, Hansen L, et al. (2021) Effect of plasticizers and polymer blends for processing softwood kraft lignin as carbon fiber precursors. *Cellulose* 28(2): 1039-1053.

Back E and Salmén L (1982) Glass transitions of wood components hold implications for molding and pulping processes. *TAPPI Journal* 65(7): 107-110.

Balakshin M and Capanema E (2015) On the Quantification of Lignin Hydroxyl Groups With 31P and 13C NMR Spectroscopy. *Journal of Wood Chemistry and Technology* 35(3): 220-237.

Balakshin M, Capanema E and Berlin A (2014) Chapter 4 - Isolation and Analysis of Lignin–Carbohydrate Complexes Preparations with Traditional and Advanced Methods: A Review. In: Atta-ur R (ed) *Studies in Natural Products Chemistry*. Elsevier, pp.83-115.

Balakshin MY, Capanema EA, Chen, et al. (2003) Elucidation of the Structures of Residual and Dissolved Pine Kraft Lignins Using an HMQC NMR Technique. *Journal of Agricultural and Food Chemistry* 51(21): 6116-6127.

Banu D, El-Aghoury A and Feldman D (2006) Contributions to characterization of poly(vinyl chloride)–lignin blends. *Journal of Applied Polymer Science* 101(5): 2732-2748.

Bardet M, Gerbaud G, Trân Q-K, et al. (2007) Study of interactions between polyethylene glycol and archaeological wood components by 13C high-resolution solid-state CP-MAS NMR. *Journal of Archaeological Science* 34(10): 1670-1676.

Barral L, Cano J, López A, et al. (1994) Determination of the activation energies for α and β transitions of a system containing a diglycidyl ether of bisphenol a

(DGEBA) and 1,3-bisaminomethylcyclohexane (1,3-BAC). *Journal of Thermal Analysis and Calorimetry* 41(6): 1463-1467.

Berglund J, Mikkelsen D, Flanagan BM, et al. (2020) Wood hemicelluloses exert distinct biomechanical contributions to cellulose fibrillar networks. *Nature Communications* 11(1): 4692.

Bertaud F and Holmbom B (2004) Chemical composition of earlywood and latewood in Norway spruce heartwood, sapwood and transition zone wood. *Wood Science and Technology* 38(4): 245-256.

Biroli G and Garrahan JP (2013) Perspective: The glass transition. *The Journal of Chemical Physics* 138(12).

Bishai AM, Gamil FA, Awni FA, et al. (1985) Dielectric and mechanical properties of poly(vinyl chloride)–dioctylphthalate systems. *Journal of Applied Polymer Science* 30(5): 2009-2020.

Björkman A (1956) Studies on finely divided wood. Part 1. Extraction of lignin with neutral solvents. *Svensk papperstidning* 59(13): 477-485.

Björn L (2025) *Synchrotron Imaging of Synthetic and Lignocellulose-based Packaging Materials*. PhD thesis, Chalmers University of Technology, Göteborg.

Bouajila J, Dole P, Joly C, et al. (2006) Some laws of a lignin plasticization. *Journal of Applied Polymer Science* 102(2): 1445-1451.

Brauns F (1939) Native lignin1 I. Its isolation and methylation. *Journal of the American Chemical Society* 61(8): 2120-2127.

Brewer MJ, Butler A and Cooksley SL (2016) The relative performance of AIC, AICC and BIC in the presence of unobserved heterogeneity. *Methods in Ecology and Evolution* 7(6): 679-692.

Browning BL (1967) *Methods of wood chemistry*. New York: Wiley, pp.720-726.

Brändström J (2002) *Morphology of Norway spruce tracheids with emphasis on cell wall organisation*. PhD thesis, Sveriges lantbruksuniversitet, Uppsala.

Bränvall E, Larsson PT and Stevanic JS (2021) Changes in the cellulose fiber wall supramolecular structure during the initial stages of chemical treatments of wood evaluated by NMR and X-ray scattering. *Cellulose* 28(7): 3951-3965.

Cavagna A (2009) Supercooled liquids for pedestrians. *Physics Reports* 476(4): 51-124.

Cavailles J, Vaca-Medina G, Wu-Tiu-Yen J, et al. (2024) Influence of Thermocompression Conditions on the Properties and Chemical Composition of Bio-Based Materials Derived from Lignocellulosic Biomass. *Materials* 17(8): 1713.

Chen W, Lickfield GC and Yang CQ (2004) Molecular modeling of cellulose in amorphous state. Part I: model building and plastic deformation study. *Polymer* 45(3): 1063-1071.

Chowdhury S and Frazier CE (2013) Thermorheological Complexity and Fragility in Plasticized Lignocellulose. *Biomacromolecules* 14(4): 1166-1173.

Clauss MM, Weldin DL, Frank E, et al. (2015) Size-Exclusion Chromatography and Aggregation Studies of Acetylated Lignins in N,N-Dimethylacetamide in the Presence of Salts. *Macromolecular Chemistry and Physics* 216(20): 2012-2019.

Cosgrove DJ, Dupree P, Gomez ED, et al. (2024) How Many Glucan Chains Form Plant Cellulose Microfibrils? A Mini Review. *Biomacromolecules* 25(10): 6357-6366.
Crestini C, Lange H, Sette M, et al. (2017) On the structure of softwood kraft lignin. *Green Chemistry* 19(17): 4104-4121.
Daicho K, Fujisawa S, Doi Y, et al. (2025) Uniform elementary fibrils in diverse plant cell walls. *Proceedings of the National Academy of Sciences* 122(15): e2426467122.
Donaldson L (2008) Microfibril angle: measurement, variation and relationships–a review. *IAWA journal* 29(4): 345-386.
Donaldson LA (2019) Wood cell wall ultrastructure the key to understanding wood properties and behaviour. *IAWA journal* 40(4): 645-672.
Donaldson LA (2022) Super-resolution imaging of Douglas fir xylem cell wall nanostructure using SRRF microscopy. *Plant Methods* 18(1): 27.
Duchesne I and Daniel G (1999) The ultrastructure of wood fibre surfaces as shown by a variety of microscopical methods – a review. *Nordic Pulp & Paper Research Journal* 14(2): 129-139.
Duchesne I, Hult E, Molin U, et al. (2001) The influence of hemicellulose on fibril aggregation of kraft pulp fibres as revealed by FE-SEM and CP/MAS 13C-NMR. *Cellulose* 8(2): 103-111.
Duval A, Vilaplana F, Crestini C, et al. (2016) Solvent screening for the fractionation of industrial kraft lignin. *Holzforschung* 70(1): 11-20.
Ebrahimi Majdar R, Ghasemian A, Resalati H, et al. (2019) Facile Isolation of LCC-Fraction from Organosolv Lignin by Simple Soxhlet Extraction. *Polymers* 11(2): 225.
Ebrahimi Majdar R, Ghasemian A, Resalati H, et al. (2020) Case Study in Kraft Lignin Fractionation: "Structurally Purified" Lignin Fractions—The Role of Solvent H-Bonding Affinity. *ACS Sustainable Chemistry & Engineering* 8(45): 16803-16813.
Ediger MD (2000) Spatially heterogeneous dynamics in supercooled liquids. *Annual Review of Physical Chemistry* 51(1): 99-128.
Ek R, Wormald P, Östelius J, et al. (1995) Crystallinity index of microcrystalline cellulose particles compressed into tablets. *International Journal of Pharmaceutics* 125(2): 257-264.
El Hachem C, Abahri K, Leclerc S, et al. (2020) NMR and XRD quantification of bound and free water interaction of spruce wood fibers. *Construction and Building Materials* 260: 120470.
Elf P (2025) *Prediction of Thermoplasticity in Lignocellulose-Based Materials using Molecular Simulations*. PhD thesis, Kungliga Tekniska högskolan, Stockholm.
Elf P, Mattsson A, Paajanen A, et al. (2025) Role of Lignin in Hot-Pressing of Paper: Insights from Molecular Simulations and Experiments. *Biomacromolecules* 26(9): 5965-5978.
Elf P, Özeren HD, Larsson PA, et al. (2023) Molecular Dynamics Simulations of Cellulose and Dialcohol Cellulose under Dry and Moist Conditions. *Biomacromolecules* 24(6): 2706-2720.

Eliasson A (2025) *Ductile wood fiber-based materials through sonication and plasticization*. PhD thesis, Kungliga Tekniska högskolan, Stockholm.
Eliasson A, Hedenqvist M, Brolin A, et al. (2023) Highly Ductile Cellulose-Rich Papers Obtained by Ultrasonication-Assisted Incorporation of Low Molecular Weight Plasticizers. *ACS Sustainable Chemistry & Engineering* 11(24): 8836-8846.
Eliasson A, Polisetti V, Hedenqvist M, et al. (2025) Pulp fiber-based composites with plasticized starch via high-shear mixing. *Carbohydrate Polymer Technologies and Applications*. 100971.
Espinoza-Acosta JL, Torres-Chávez PI, Carvajal-Millán E, et al. (2014) Ionic liquids and organic solvents for recovering lignin from lignocellulosic biomass. *BioResources* 9(2).
Esteban LG, de Palacios P, Heinz I, et al. (2023) Softwood Anatomy: A Review. *Forests* 14(2): 323.
Fahlén J and Salmén L (2002) On the Lamellar Structure of the Tracheid Cell Wall. *Plant Biology* 4(3): 339-345.
Fahlén J and Salmén L (2003) Cross-sectional structure of the secondary wall of wood fibers as affected by processing. *Journal of Materials Science* 38(1): 119-126.
Faix O, Argyropoulos DS, Robert D, et al. (1994) Determination of Hydroxyl Groups in Lignins Evaluation of 1H-, 13C-, 31P-NMR, FTIR and Wet Chemical Methods. *Holzforschung* 48(5): 387-394.
Faleva AV, Belesov AV, Kozhevnikov AY, et al. (2021) Analysis of the functional group composition of the spruce and birch phloem lignin. *International Journal of Biological Macromolecules* 166: 913-922.
Fernando D, Kowalczyk M, Guindos P, et al. (2023) Electron tomography unravels new insights into fiber cell wall nanostructure; exploring 3D macromolecular biopolymeric nano-architecture of spruce fiber secondary walls. *Scientific Reports* 13(1): 2350.
Ferrer ML, Lawrence C, Demirjian BG, et al. (1998) Supercooled liquids and the glass transition: Temperature as the control variable. *The Journal of Chemical Physics* 109(18): 8010-8015.
Fox SC and McDonald AG (2010) Chemical and thermal characterization of three industrial lignins and their corresponding lignin esters. *BioResources* 5(2): 990-1009.
Fox TG and Flory PJ (1954) The glass temperature and related properties of polystyrene. Influence of molecular weight. *Journal of Polymer Science* 14(75): 315-319.
Fox TG, Jr. and Flory PJ (1950) Second-Order Transition Temperatures and Related Properties of Polystyrene. I. Influence of Molecular Weight. *Journal of Applied Physics* 21(6): 581-591.
Froass PM, Ragauskas AJ and Jiang J-E (1996) Chemical Structure of Residual Lignin from Kraft Pulp. *Journal of Wood Chemistry and Technology* 16(4): 347-365.
Fromm J, Rockel B, Lautner S, et al. (2003) Lignin distribution in wood cell walls determined by TEM and backscattered SEM techniques. *Journal of Structural Biology* 143(1): 77-84.

Gama N, Santos R, Godinho B, et al. (2019) Triacetin as a Secondary PVC Plasticizer. *Journal of Polymers and the Environment* 27(6): 1294-1301.

Garvey C, Parker I and Simon G (2005) On the Interpretation of X-Ray Diffraction Powder Patterns in Terms of the Nanostructure of Cellulose I Fibres. *Macromolecular Chemistry and Physics* 206: 1568-1575.

Gellerstedt G and Zhang L (2001) Chemistry of TCF-Bleaching with Oxygen and Hydrogen Peroxide. In: Argyropoulos DS (ed) *Oxidative Delignification Chemistry*. Washington, D.C.: American Chemical Society, pp.61-72.

Gezici-Koç Ö, Erich SJF, Huinink HP, et al. (2017) Bound and free water distribution in wood during water uptake and drying as measured by 1D magnetic resonance imaging. *Cellulose* 24(2): 535-553.

Ghaffari R, Almqvist H, Idström A, et al. (2023) Effect of alkalinity on the diffusion of solvent-fractionated lignin through cellulose membranes. *Cellulose* 30(6): 3685-3698.

Gioia C, Lo Re G, Lawoko M, et al. (2018) Tunable Thermosetting Epoxies Based on Fractionated and Well-Characterized Lignins. *Journal of the American Chemical Society* 140(11): 4054-4061.

Giummarella N, Pu Y, Ragauskas AJ, et al. (2019) A critical review on the analysis of lignin carbohydrate bonds. *Green Chemistry* 21(7): 1573-1595.

Goring DAI (1963) Thermal softening of lignin, hemicellulose and cellulose. *Pulp Paper Mag. Can.* 64(12): T517-T527.

Gravitis J, Kokorevics A, Zharov A, et al. (1991) Simultaneous Action of Shear Deformation and High Pressure. *Journal of pulp and paper science* 17(4).

Guerra A, Filpponen I, Lucia LA, et al. (2006a) Comparative Evaluation of Three Lignin Isolation Protocols for Various Wood Species. *Journal of Agricultural and Food Chemistry* 54(26): 9696-9705.

Guerra A, Filpponen I, Lucia LA, et al. (2006b) Toward a Better Understanding of the Lignin Isolation Process from Wood. *Journal of Agricultural and Food Chemistry* 54(16): 5939-5947.

Guerra A, Gaspar AR, Contreras S, et al. (2007) On the propensity of lignin to associate: A size exclusion chromatography study with lignin derivatives isolated from different plant species. *Phytochemistry* 68(20): 2570-2583.

Hackenstrass K, Hasani M and Wohlert M (2024) Structure, flexibility and hydration properties of lignin dimers studied with Molecular Dynamics simulations. *Holzforschung* 78(2): 98-108.

Hackenstrass K, Tabudlong Jonasson N, Hartwig-Nair M, et al. (2025) Analysing π-π-stacking interactions in lignin nanoparticles from molecular simulations – insights and lessons learned. *Faraday Discussions*. DOI: 10.1039/d5fd00052a.

Hagen R, Salmén L, Lavebratt H, et al. (1994) Comparison of dynamic mechanical measurements and Tg determinations with two different instruments. *Polymer Testing* 13(2): 113-128.

Hancock BC and Zografi G (1994) The Relationship Between the Glass Transition Temperature and the Water Content of Amorphous Pharmaceutical Solids. *Pharmaceutical Research* 11(4): 471-477.

Hanley SJ and Gray DG (1994) Atomic Force Microscope Images of Black Spruce Wood Sections and Pulp Fibres. 48(1): 29-34.
Hansen CM (2000) *Hansen solubility parameters : a user's handbook*. Boca Raton, Fla.: CRC Press.
Hashimoto T, Kawamura T, Harada M, et al. (1994) Small-Angle Scattering from Hexagonally Packed Cylindrical Particles with Paracrystalline Distortion. *Macromolecules* 27(11): 3063-3072.
Havimo M (2009) A literature-based study on the loss tangent of wood in connection with mechanical pulping. *Wood Science and Technology* 43(7): 627-642.
Hawkes GE, Smith CZ, Utley JH, et al. (1993) A comparison of solution and solid state 13C NMR spectra of lignins and lignin model compounds.
Heituer C and Atack D (1984) Dynamic mechanical properties of sulphite treated aspen. *Paperi ju Puu* 66(2): 84–89.
Henrik-Klemens Å (2023) *Viscoelastic Properties and Plasticization Potential of Native Residual and Technical Lignin*. Licentiate thesis, Chalmers Tekniska högskola Göteborg.
Henriksson G, Germgård U and Lindström ME (2024) A review on chemical mechanisms of kraft pulping. *Nordic Pulp & Paper Research Journal* 39(3): 297-311.
Hill DJT, Whittaker AK and Wong KW (1999) Miscibility and Specific Interactions in Blends of Poly(4-vinylphenol) and Poly(2-ethoxyethyl methacrylate). *Macromolecules* 32(16): 5285-5291.
Härdelin L, Bernin D, Börjesson M, et al. (2020) Altered Thermal and Mechanical Properties of Spruce Galactoglucomannan Films Modified with an Etherification Reaction. *Biomacromolecules* 21(5): 1832-1840.
Iiyama K and Wallis AFA (1990) Determination of lignin in herbaceous plants by an improved acetyl bromide procedure. *Journal of the Science of Food and Agriculture* 51(2): 145-161.
Jarnerö K, Vikberg T, Sandberg K, et al. (2024) Områdesanalys för träindustrins biogena kolflöden. Stockholm: RISE Research Institutes of Sweden.
Jarvis MC (2018) Structure of native cellulose microfibrils, the starting point for nanocellulose manufacture. *Philosophical Transactions of the Royal Society A: Mathematical, Physical and Engineering Sciences* 376(2112): 20170045.
Jeoh T, Karuna N, Weiss ND, et al. (2017) Two-Dimensional 1H-Nuclear Magnetic Resonance Relaxometry for Understanding Biomass Recalcitrance. *ACS Sustainable Chemistry & Engineering* 5(10): 8785-8795.
Jeremic D, Cooper P and Brodersen P (2007) Penetration of poly(ethylene glycol) into wood cell walls of red pine. *Holzforschung* 61(3): 272-278.
Jin K, Qin Z and Buehler MJ (2015) Molecular deformation mechanisms of the wood cell wall material. *Journal of the Mechanical Behavior of Biomedical Materials* 42: 198-206.
Jääskeläinen AS, Sun Y, Argyropoulos DS, et al. (2003) The effect of isolation method on the chemical structure of residual lignin. *Wood Science and Technology* 37(2): 91-102.

Kang X, Kirui A, Dickwella Widanage MC, et al. (2019) Lignin-polysaccharide interactions in plant secondary cell walls revealed by solid-state NMR. *Nature Communications* 10(1): 347.

Karaaslan MA, Cho M, Liu L-Y, et al. (2021) Refining the Properties of Softwood Kraft Lignin with Acetone: Effect of Solvent Fractionation on the Thermomechanical Behavior of Electrospun Fibers. *ACS Sustainable Chemistry & Engineering* 9(1): 458-470.

Keckes J, Burgert I, Frühmann K, et al. (2003) Cell-wall recovery after irreversible deformation of wood. *Nature Materials* 2(12): 810-813.

Kelley SS, Rials TG and Glasser WG (1987) Relaxation behaviour of the amorphous components of wood. *Journal of Materials Science* 22(2): 617-624.

Kerr A and Goring D (1975) Ultrastructural arrangement of the wood cell wall. *Cellulose Chemistry and Technology* 9(6): 563–573.

Kesari KK, O'Reilly P, Seitsonen J, et al. (2021) Infrared photo-induced force microscopy unveils nanoscale features of Norway spruce fibre wall. *Cellulose* 28(11): 7295-7309.

Klähn M, Krishnan R, Phang JM, et al. (2019) Effect of external and internal plasticization on the glass transition temperature of (Meth)acrylate polymers studied with molecular dynamics simulations and calorimetry. *Polymer* 179: 121635.

Kulasinski K, Derome D and Carmeliet J (2017) Impact of hydration on the micromechanical properties of the polymer composite structure of wood investigated with atomistic simulations. *Journal of the Mechanics and Physics of Solids* 103: 221-235.

Kumar V and Kothari SH (1999) Effect of compressional force on the crystallinity of directly compressible cellulose excipients. *International Journal of Pharmaceutics* 177(2): 173-182.

Laschimke R (1989) Investigation of the wetting behaviour of natural lignin - a contribution to the cohesion theory of water transport in plants. *Thermochimica Acta* 151: 35-56.

Lawoko M, Berggren R, Berthold F, et al. (2004) Changes in the lignin-carbohydrate complex in softwood kraft pulp during kraft and oxygen delignification. *Holzforschung* 58(6): 603-610.

Li K and and Reeve DW (2005) Sample Contamination in Analysis of Wood Pulp Fibers with X-ray Photoelectron Spectroscopy. *Journal of Wood Chemistry and Technology* 24(3): 183-200.

Liitiä T (2002) *Application of modern NMR spectroscopic techniques to structural studies of wood and pulp components*. PhD thesis, Helsingin yliopisto, Helsinki.

Liitiä T, Maunu SL and Hortling B (2001) Solid State NMR Studies on Inhomogeneous Structure of Fibre Wall in Kraft Pulp. *Holzforschung* 55(5): 503-510.

Ling Z, Wang T, Makarem M, et al. (2019) Effects of ball milling on the structure of cotton cellulose. *Cellulose* 26(1): 305-328.

Liu Y, Roy A, Jones A, et al. (1990) An NMR study of plasticization and antiplasticization of a polymeric glass. *Macromolecules* 23(4): 968-977.

Lupoi JS, Singh S, Parthasarathi R, et al. (2015) Recent innovations in analytical methods for the qualitative and quantitative assessment of lignin. *Renewable and Sustainable Energy Reviews* 49: 871-906.

Mahlin D, Wood J, Hawkins N, et al. (2009) A novel powder sample holder for the determination of glass transition temperatures by DMA. *International Journal of Pharmaceutics* 371(1): 120-125.

Martinez CR and Iverson BL (2012) Rethinking the term "pi-stacking". *Chemical Science* 3(7): 2191-2201.

McCarthy JL and Islam A (1999) Lignin Chemistry, Technology, and Utilization: A Brief History. In: Glasser WG, Northey RA and Schultz TP (eds) *Lignin: Historical, Biological, and Materials Perspectives*. Washington, D.C.: American Chemical Society, pp.2-99.

Menard KP (2008) *Dynamic mechanical analysis : a practical introduction*. Boca Raton, Fla.: CRC Press.

Meurer B and Weill G (2008) Measurement of Spin Diffusion Coefficients in Glassy Polymers: Failure of a Simple Scaling Law. *Macromolecular Chemistry and Physics* 209(2): 212-219.

Milotskyi R, Szabó L, Takahashi K, et al. (2019) Chemical Modification of Plasticized Lignins Using Reactive Extrusion. *Frontiers in Chemistry* 7(633).

Mirau PA (2005) *A practical guide to understanding the NMR of polymers*. Hoboken, N.J.: J. Wiley, pp.280-295 & 336-369.

Miyoshi Y, Sakae A, Arimura N, et al. (2018) Temperature dependences of the dynamic viscoelastic properties of wood and acetylated wood swollen by water or organic liquids. *Journal of Wood Science* 64(2): 157-163.

Mok MM, Kim J and Torkelson JM (2008) Gradient copolymers with broad glass transition temperature regions: Design of purely interphase compositions for damping applications. *Journal of Polymer Science Part B: Polymer Physics* 46(1): 48-58.

Montanari C, Olsén P and Berglund LA (2021) Sustainable Wood Nanotechnologies for Wood Composites Processed by In-Situ Polymerization. *Frontiers in Chemistry* 9: 682883.

Månsson P (1983) Quantitative Determination of Phenolic and Total Hydroxyl Groups in Lignins. *Holzforschung* 37(3): 143-146.

Ni H, Ren S, Fang G, et al. (2016) Determination of alkali lignin solubility parameters by inverse gas chromatography and hansen solubility parameters. *BioResources* 11(2): 4353-4368.

Nicholson DJ, Duarte GV, Alves EF, et al. (2012) Preliminary Results on an Approach for the Quantification of Lignin-Carbohydrate Complexes (LCC) in Hardwood Pulps. *Journal of Wood Chemistry and Technology* 32(3): 238-252.

Nicholson DJ, Leavitt AT, Stromberg B, et al. (2017) Mechanistic Differences Between Kraft and Soda-AQ Pulping of Hardwoods with Regard to Lignin–Carbohydrate Complexes (LCC). *Journal of Wood Chemistry and Technology* 37(4): 307-322.

Nielsen LE, Buchdahl R and Levreault R (1950) Mechanical and Electrical Properties of Plasticized Vinyl Chloride Compositions. *Journal of Applied Physics* 21(6): 607-614.

Nowacka A, Mohr PC, Norrman J, et al. (2010) Polarization Transfer Solid-State NMR for Studying Surfactant Phase Behavior. *Langmuir* 26(22): 16848-16856.

Ogawa T (1992) Effects of molecular weight on mechanical properties of polypropylene. *Journal of Applied Polymer Science* 44(10): 1869-1871.

Okugawa A, Yuguchi Y and Yamane C (2023) Dynamic viscoelastic behavior of natural cellulose fibers caused by water and the related swelling phenomenon. *Cellulose* 30(7): 4149-4158.

Oliaei E, Berthold F, Berglund LA, et al. (2021) Eco-Friendly High-Strength Composites Based on Hot-Pressed Lignocellulose Microfibrils or Fibers. *ACS Sustainable Chemistry & Engineering* 9(4): 1899-1910.

Oliaei E, Lindén PA, Wu Q, et al. (2020) Microfibrillated lignocellulose (MFLC) and nanopaper films from unbleached kraft softwood pulp. *Cellulose* 27(4): 2325-2341.

Olsson A-M and Salmén L (1997) The effect of lignin composition on the viscoelastic properties of wood. *Nordic Pulp & Paper Research Journal* 12(3): 140-144.

Oram BK, Monu and Bandyopadhyay B (2020) Impact of donor acidity and acceptor anharmonicity on vc=o spectral shifts in O-H···O=C H-bonded ketone-alcohol complexes: An IR spectroscopic investigation. *Spectrochimica Acta Part A: Molecular and Biomolecular Spectroscopy* 230: 118070.

Paajanen A, Zitting A, Rautkari L, et al. (2022) Nanoscale Mechanism of Moisture-Induced Swelling in Wood Microfibril Bundles. *Nano Letters* 22(13): 5143-5150.

Paes SS, Sun S, MacNaughtan W, et al. (2010) The glass transition and crystallization of ball milled cellulose. *Cellulose* 17(4): 693-709.

Parit M and Jiang Z (2020) Towards lignin derived thermoplastic polymers. *International Journal of Biological Macromolecules* 165: 3180-3197.

Penttila PA, Rautkari L, Osterberg M, et al. (2019) Small-angle scattering model for efficient characterization of wood nanostructure and moisture behaviour. *Journal of Applied Crystallography* 52(2): 369-377.

Penttilä PA, Altgen M, Awais M, et al. (2020) Bundling of cellulose microfibrils in native and polyethylene glycol-containing wood cell walls revealed by small-angle neutron scattering. *Scientific Reports* 10(1): 20844.

Penvern H, Zhou M, Maillet B, et al. (2020) How Bound Water Regulates Wood Drying. *Physical Review Applied* 14(5): 054051.

Pereira A, Hoeger IC, Ferrer A, et al. (2017) Lignin Films from Spruce, Eucalyptus, and Wheat Straw Studied with Electroacoustic and Optical Sensors: Effect of Composition and Electrostatic Screening on Enzyme Binding. *Biomacromolecules* 18(4): 1322-1332.

Pesquet E, Cesarino I, Kajita S, et al. (2025) Physiological roles of lignins – tuning cell wall hygroscopy and biomechanics. *New Phytologist* 248(6): 2674-2706.

Petridis L and Smith JC (2016) Conformations of Low-Molecular-Weight Lignin Polymers in Water. *ChemSusChem* 9(3): 289-295.

Pettersson G, Norgren S and Höglund H (2017) Strong paper from spruce CTMP - Part I. *Nordic Pulp & Paper Research Journal* 32(1): 54-58.
Pintiaux T, Heuls M, Vandenbossche V, et al. (2019) Cellulose consolidation under high-pressure and high-temperature uniaxial compression. *Cellulose* 26(5): 2941-2954.
Polčin J and Bezúch B (1978) Enzymic isolation of lignin from wood and pulps. *Wood Science and Technology* 12(2): 149-158.
Ralph J, Lapierre C and Boerjan W (2019) Lignin structure and its engineering. *Current Opinion in Biotechnology* 56: 240-249.
Reza M, Bertinetto C, Ruokolainen J, et al. (2017) Cellulose Elementary Fibrils Assemble into Helical Bundles in S1 Layer of Spruce Tracheid Wall. *Biomacromolecules* 18(2): 374-378.
Roe R-J (2000) *Methods of X-ray and neutron scattering in polymer science.* New York: Oxford Univ. Press, pp.82-98 & 155-157.
Rowell R (2013) *Handbook of wood chemistry and wood composites.* Boca Raton: CRC.
Ruel K, Barnoud F and Goring DAI (1978) Lamellation in the S2 layer of softwood tracheids as demonstrated by scanning transmission electron microscopy. *Wood Science and Technology* 12(4): 287-291.
Sadoh T (1981) Viscoelastic properties of wood in swelling systems. *Wood Science and Technology* 15(1): 57-66.
Sakata I and Senju R (1975) Thermoplastic behavior of lignin with various synthetic plasticizers. *Journal of Applied Polymer Science* 19(10): 2799-2810.
Salem KS, Kasera NK, Rahman MA, et al. (2023) Comparison and assessment of methods for cellulose crystallinity determination. *Chemical Society Reviews* 52(18): 6417-6446.
Salmén L (1982) *Temperature and water induced softening behaviour of wood fiber based materials*. PhD thesis, Kungliga Tekniska högskolan, Stockholm.
Salmén L (1984) Viscoelastic properties ofin situ lignin under water-saturated conditions. *Journal of Materials Science* 19(9): 3090-3096.
Salmén L (2004) Micromechanical understanding of the cell-wall structure. *Comptes Rendus Biologies* 327(9): 873-880.
Salmén L (2018) Wood Cell Wall Structure and Organisation in Relation to Mechanics. In: Geitmann A and Gril J (eds) *Plant Biomechanics: From Structure to Function at Multiple Scales*. Cham: Springer International Publishing, pp.3-19.
Salmén L (2022) On the organization of hemicelluloses in the wood cell wall. *Cellulose* 29(3): 1349-1355.
Salmén L, Back E and Alwarsdotter Y (1984) Effects of Non-Aqueous Plasticizers on the Thermal Softening of Paper. *Journal of Wood Chemistry and Technology* 4(3): 347-365.
Salmén L, Stevanic JS and Olsson A-M (2016) Contribution of lignin to the strength properties in wood fibres studied by dynamic FTIR spectroscopy and dynamic mechanical analysis (DMA). *Holzforschung* 70(12): 1155-1163.
Sameni J, Krigstin S and Sain M (2017) Solubility of lignin and acetylated lignin in organic solvents. *BioResources* 12(1): 1548-1565.

Sanchez-Salvador JL, Pettersson G, Mattsson A, et al. (2024) Extending the limits of using chemithermomechanical pulp by combining lignin microparticles and hot-pressing technology. *Cellulose* 31(15): 9335-9348.
Sapouna I and Lawoko M (2021) Deciphering lignin heterogeneity in ball milled softwood: unravelling the synergy between the supramolecular cell wall structure and molecular events. *Green Chemistry* 23(9): 3348-3364.
Schaefer J, Garbow JR, Stejskal E, et al. (1987) Plasticization of poly (butyral-covinyl alcohol). *Macromolecules* 20(6): 1271-1278.
Segal L, Creely, J.J., Martin Jr., A.E. and Conrad, C.M. (1959) An Empirical Method for Estimating the Degree of Crystallinity of Native Cellulose Using the X-Ray Diffractometer. *Textile Research Journal* 29: 786-794.
Sjöström E (1981) *Wood chemistry : fundamentals and applications*. New York: Academic P.
Song P and Wang H (2020) High-Performance Polymeric Materials through Hydrogen-Bond Cross-Linking. *Advanced Materials* 32(18): 1901244.
Souto F and Calado V (2022) Mystifications and misconceptions of lignin: revisiting understandings. *Green Chemistry* 24(21): 8172-8192.
Startsev OV, Makhonkov A, Erofeev V, et al. (2017) Impact of moisture content on dynamic mechanical properties and transition temperatures of wood. *Wood Material Science & Engineering* 12(1): 55-62.
Stukalin EB, Douglas JF and Freed KF (2010) Plasticization and antiplasticization of polymer melts diluted by low molar mass species. *The Journal of Chemical Physics* 132(8): 084504.
Sun Y and Sun G (2024) A natural butter glyceride as a plasticizer for improving thermal, mechanical, and biodegradable properties of poly(lactide acid). *International Journal of Biological Macromolecules* 263: 130366.
Szcześniak L, Rachocki A and Tritt-Goc J (2008) Glass transition temperature and thermal decomposition of cellulose powder. *Cellulose* 15(3): 445-451.
Tai H-C, Chang C-H, Cai W, et al. (2023) Wood cellulose microfibrils have a 24-chain core–shell nanostructure in seed plants. *Nature Plants* 9(7): 1154-1168.
Terashima N, Kitano K, Kojima M, et al. (2009) Nanostructural assembly of cellulose, hemicellulose, and lignin in the middle layer of secondary wall of ginkgo tracheid. *Journal of Wood Science* 55(6): 409-416.
Terrett OM, Lyczakowski JJ, Yu L, et al. (2019) Molecular architecture of softwood revealed by solid-state NMR. *Nature Communications* 10(1): 4978.
Testova L, Borrega M, Tolonen LK, et al. (2014) Dissolving-grade birch pulps produced under various prehydrolysis intensities: quality, structure and applications. *Cellulose* 21(3): 2007-2021.
Thybring EE, Fredriksson M, Zelinka SL, et al. (2022) Water in Wood: A Review of Current Understanding and Knowledge Gaps. *Forests* 13(12): 2051.
Tian X, Wang B, Wang B, et al. (2017) Structural characterization of lignin isolated from wheat-straw during the alkali cooking process. *BioResources* 12(2): 2407-2420.

Tsioptsias C (2021) Glass chemical transition: An unknown thermal transition observed in cellulose acetate butyrate. *Carbohydrate Polymers* 259: 117754.
Vaca-Medina G, Jallabert B, Viet D, et al. (2013) Effect of temperature on high pressure cellulose compression. *Cellulose* 20(5): 2311-2319.
Vikström B and Nelson P (1980) Mechanical properties of chemically treated wood and chemimechanical pulps. *TAPPI Journal* 63(3): 87-91.
Vilics T, Schneider HA, Manoviciu V, et al. (1997) A new approach to PVC-plasticizer interaction by using a Tg concentration power equation. *Polymer* 38(8): 1865-1870.
Virtanen T, Penttilä PA, Maloney TC, et al. (2015) Impact of mechanical and enzymatic pretreatments on softwood pulp fiber wall structure studied with NMR spectroscopy and X-ray scattering. *Cellulose* 22(3): 1565-1576.
Vishtal A and Retulainen E (2014) Boosting the extensibility potential of fibre networks: A review. *BioResources* 9(4): 7951-8001.
Vural D, Gainaru C, O'Neill H, et al. (2018a) Impact of hydration and temperature history on the structure and dynamics of lignin. *Green Chemistry* 20(7): 1602-1611.
Vural D, Smith JC and Petridis L (2018b) Dynamics of the lignin glass transition. *Physical Chemistry Chemical Physics* 20(31): 20504-20512.
Wang C, Kelley SS and Venditti RA (2016) Lignin-Based Thermoplastic Materials. *ChemSusChem* 9(8): 770-783.
Weng JK and Chapple C (2010) The origin and evolution of lignin biosynthesis. *New Phytologist* 187(2): 273-285.
Wu G, Liu Y and Shi G (2021) New Experimental Evidence for Thermodynamic Links to the Kinetic Fragility of Glass-Forming Polymers. *Macromolecules* 54(12): 5595-5606.
Wu S and Argyropoulos D (2003) An improved method for lsolating lignin in high yield and purity. *Journal of pulp and paper science* 29(7): 235-240.
Yoshida H, Mörck R, Kringstad KP, et al. (1987) Fractionation of Kraft Lignin by Successive Extraction with Organic Solvents. II. Thermal Properties of Kraft Lignin Fractions. *Holzforschung* 41(3): 171-176.
Zhang C, Chen M, Keten S, et al. (2021) Hygromechanical mechanisms of wood cell wall revealed by molecular modeling and mixture rule analysis. *Science Advances* 7(37): eabi8919.
Zhang L, Larsson A, Moldin A, et al. (2022) Comparison of lignin distribution, structure, and morphology in wheat straw and wood. *Industrial Crops and Products* 187: 115432.
Zhang Y, Yu J and Cosgrove DJ (2025) Mechanical Roles of Polysaccharide Assembly and Interactions in Plant Cell Walls. *Biomacromolecules* 26(8): 5010-5019.
Zinovyev G, Sulaeva I, Podzimek S, et al. (2018) Getting Closer to Absolute Molar Masses of Technical Lignins. *ChemSusChem* 11(18): 3259-3268.
Åkerholm M and Salmén L (2004) Softening of wood polymers induced by moisture studied by dynamic FTIR spectroscopy. *Journal of Applied Polymer Science* 94(5): 2032-2040.

Özeren HD, Guivier M, Olsson RT, et al. (2020) Ranking Plasticizers for Polymers with Atomistic Simulations: PVT, Mechanical Properties, and the Role of Hydrogen Bonding in Thermoplastic Starch. *ACS Applied Polymer Materials* 2(5): 2016-2026.

Appended papers